Science of the Total Environment 1025 (2026) 181659

Contents lists available at ScienceDirect

Science of the Total Environment

journal homepage: www.elsevier.com/locate/scitotenv

Microbial dispersal from a hyperactive sandsheet in the Icelandic Highland

Nathan Hadland [a], Christopher W. Hamilton [a], Peter Schroedl [b], Federica Calabrese [b], Jeffery Marlow [b], Solange Duhamel [a,c,*]

[a] The University of Arizona, Lunar and Planetary Laboratory, Tucson, AZ, 85721, USA
[b] Boston University, Department of Biology, 5 Cummington Mall, Boston, MA, 02215, USA
[c] The University of Arizona, Molecular and Cellular Biology, Tucson, AZ, 85721, USA

HIGHLIGHTS

- Bioaerosols from an Arctic dust hotspot linked to local surfaces and storm events.
- Source tracking shows aerosols have microbes from sand, floodplains, and glaciers.
- Wind speed and pressure drive airborne diversity and phylogenetic clustering.
- Microscopy reveals microbes are preferentially attached to opaque/complex grains.
- Findings highlight Arctic dust as a vector for potentially pathogenic microbess.

GRAPHICAL ABSTRACT

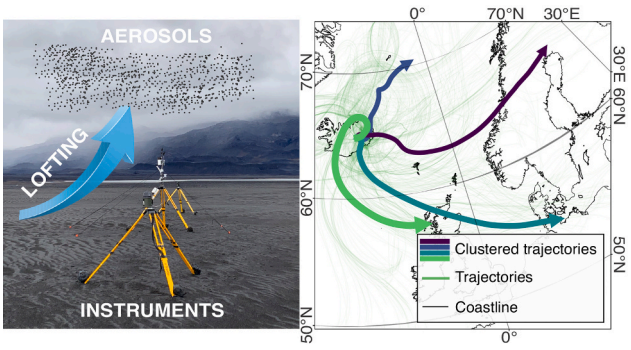

ARTICLE INFO

Dataset link: Microbial Dispersal from a Hyperactive Sandsheet in the Icelandic Highlands (Original data)

Keywords:
Iceland
Bioaerosol
Bacteria
Particulate matter
Microbial emission

ABSTRACT

Atmospheric transport is an important mechanism for microbial dispersal around the world. Consequently, the coupling of atmospheric and soil ecosystems plays an important role in the global biosphere and biogeochemical cycles. We use the hyperactive Dyngjusandur sandsheet in the Icelandic highlands, a significant contributor to the global dust cycle, as a case study to link bioaerosol communities to local surface sources and show how meteorological conditions shape the dynamics of airborne microorganisms. Our findings reveal that the atmosphere over this sandsheet contains a unique community, whose structure responds dynamically to wind speed and atmospheric pressure, specifically major storm systems that alter both prokaryotic and eukaryotic populations. Source tracking revealed that storm events increased the contribution of sand-associated microorganisms to the atmosphere (up to 76%), blurring the distinction between airborne communities and their terrestrial sources—including sand, diurnal floodplains, and fluvial environments. Microorganisms were preferentially attached to morphologically complex dust particles emitted from the sandsheet, potentially increasing survivability in the atmosphere. Culturing confirmed the presence of viable, cold-adapted and stress-tolerant taxa, suggesting potential for atmospheric persistence. Forward trajectory modelling suggests that bioaerosols emitted from the sandsheet could reach major population centers in Europe. Those microorganisms could have impacts on human health, agriculture, biogeochemical cycles, and ecosystems.

* Corresponding author at: The University of Arizona, Lunar and Planetary Laboratory, Tucson, AZ, 85721, USA.
E-mail address: duhamel@arizona.edu (S. Duhamel).

https://doi.org/10.1016/j.scitotenv.2026.181659
Received 15 August 2025; Received in revised form 2 March 2026; Accepted 4 March 2026
Available online 10 March 2026
0048-9697/© 2026 Elsevier B.V. All rights are reserved, including those for text and data mining, AI training, and similar technologies.

1. Introduction

Aerosols are widespread in the atmosphere and have profound impacts on the biosphere and public health (Kim et al., 2018). Airborne microorganisms in particular influence global climate through cloud and precipitation formation, contribute to biogeochemical cycles and atmospheric chemistry, and can be transported across continents (Fröhlich-Nowoisky et al., 2016). Despite their significance, the atmospheric microbiome remains one of the least explored frontiers in extremophile research. The atmosphere can be a harsh environment for microorganisms, characterized by desiccation, oxidizing conditions, limited nutrients, and ultraviolet radiation. These stressors challenge microbial survival and dispersal, and pose technical difficulties in studying airborne communities due to low biomass (Smith et al., 2011). While many of these atmospheric conditions are bactericidal, dust can offer some protection, and microbial viability may depend on whether cells are free-floating or particle-attached, as well as on the properties of the particles themselves (Dong et al., 2022; Hu et al., 2020). Consequently, studying hyperactive dust-emitting environments—those with frequent and intense emissions—is critical for understanding microbial transport on local and global scales.

Airborne biological particles facilitate the movement of plant and microbial materials across geographical barriers, enabling genetic exchange between isolated habitats and contribute to ecosystem development, evolution, and resilience (Womack et al., 2010), but transported microorganisms may also be allergy triggers, affect agriculture, or be pathogenic (Fröhlich-Nowoisky et al., 2016). Despite these implications for human health and the biosphere, little is known about the interaction between near-surface soil communities, the atmosphere, and dust storms. While previous research has linked sediment in arid environments to bioaerosol emission using sediment transport modelling (Carotenuto et al., 2017), few studies have systematically linked atmospheric microbial populations to their emission sources (Niu et al., 2023; Qi et al., 2020).

Large seasonal dust pulses from African and Asian deserts have impacts on downwind ecosystems, transporting microorganisms, including fungi and human and animal pathogens (Kellogg and Griffin, 2006; Pointing and Belnap, 2012). For example, dust-associated fungi have been implicated in coral reef decline (Weir-Brush et al., 2004), highlighting the relevance of long-range microbial transport to environmental change globally. However, far less attention has been given to high-latitude dust sources. In particular, Icelandic deserts and glacial sediments constitute the largest source of airborne dust to mainland Europe and are major contributors to the global dust cycle (Arnalds et al., 2016; Bullard et al., 2016). Iceland contains over 20,000 km^2 of sandy semi-arid deserts that are mostly composed of basaltic glass and lithic fragments, with several hyperactive dust producing hotspots (Baratoux et al., 2011). These dust emissions are likely increasing with the retreat of glaciers (Bullard et al., 2016), potentially enhancing microbial dispersal, including pathogens identified in glacial communities (Yarzábal et al., 2021; Zhang et al., 2024). Beyond human health risks, dust emission can affect the climate by reducing snow albedo (Meinander et al., 2014) and the high iron content (~10% Fe) in volcanic dust has been shown to disrupt oceanic biogeochemical processes in the North Atlantic upon deposition (Achterberg et al., 2018). Advancing desert sandsheets in Iceland also threaten the fragile ecological balance of the island (Arnalds et al., 2016; Baratoux et al., 2011).

Predicting the origin of airborne microorganisms requires comparing atmospheric communities with potential source habitats. Dominant sources of microorganisms to the atmosphere can include soil, water bodies, leaf/plant, animal feces, and anthropogenic environments (Niu et al., 2023; Qi et al., 2020). While previous work has attempted to infer the provenance of species identified in aerosols (Bowers et al., 2011), rigorous statistical approaches (Knights et al., 2011) leveraging samples collected from potential sources in the study area have rarely been employed in the natural environment (Niu et al., 2023; Qi et al., 2020; Uetake et al., 2019). Moreover, entrainment of bioaerosols is strongly associated with environmental factors such as solar irradiance and temperature (Gusareva et al., 2019), or mechanical disturbance of surfaces by wind and rainfall (Joung et al., 2017). Meteorological conditions additionally influence the diversity of airborne microbial communities in natural environments through environmental filtering (Bowers et al., 2013; Ruiz-Gil et al., 2020), which generally contrasts with urban areas where pollutants shape the community composition (Qi et al., 2020). However, most studies rely on distant weather stations rather than site-specific measurements, which may poorly represent local conditions (De Frenne et al., 2025).

Here, we use the Dyngjusandur sandsheet—a well-characterized glaciofluvial plain in the Icelandic highland (Arnalds et al., 2016; Baratoux et al., 2011; Hudziak et al., 2025) where daily katabatic winds from the Vatnajökull ice sheet drive frequent dust storms—as a case study to address three central questions about microbial dispersal from high-latitude dust sources: (1) How do meteorological conditions control the structure and diversity of local airborne microbial communities? (2) Can atmospheric microorganisms be traced to specific source environments, and does this attribution change with weather conditions? (3) Are transported microorganisms viable and associated with dust particles in ways that may enhance atmospheric survival? To answer these questions, we combine high-resolution local meteorological data with biological sampling to understand the conditions driving microbial dispersal. We characterize the atmospheric microbial community composition and diversity through amplicon sequencing of 16S and 18S rRNA genes and evaluate the relationship between microbial diversity and meteorological parameters. We further assess the role of environmental filtering in shaping airborne communities and investigate their provenance by comparing bioaerosols to potential sources in the study area (sand, diurnal floodplain sediment, and water) using both qualitative (overlap of taxa and beta diversity) and quantitative (Bayesian source tracking) methods. The viability of transported microorganisms is confirmed through culture-based isolations, while microscopy visualizes associations between microbial cells and dust particles that may enhance atmospheric survival. Collectively, these complementary approaches provide a rigorous assessment of how local environmental conditions drive microbial dispersal dynamics in a hyperactive dust environment, with implications for understanding ecosystem connectivity and potential health risks as glacial retreat intensifies high-latitude dust emissions (Bullard et al., 2016).

2. Materials and methods

2.1. Field site

The Dyngjusandur sandsheet, bordered to the northwest by the Askja central volcano and to the east by the major glacial drainage system of the Jökulsá á Fjöllum and by the Vaðalda shield volcano (Fig. 1), is a large glaciofluvial plain. The sandsheet formed from hyaloclastite silt deposition caused by diurnal flooding and jökulhlaups (massive outburst flooding) from the Dyngjujökull outlet glacier of Vatnajökull (Baratoux et al., 2011; Mountney and Russell, 2004), as well as from volcanic tephra from the nearby Askja, Kverkjöll, and Bárðarbunga volcanic systems. Areas of the sandsheet have diurnal flooding patterns in the summer—it floods in the afternoon and dries out overnight because it is situated in the rain shadow of the Vatnajökull ice sheet, resulting in a semi-arid environment. Consequently, dust storms often occur daily due to prevailing southwesterly katabatic winds descending from Vatnajökull and lofting the dried sediment. Dyngjusandur is covered in snow for most of the year, so dust emission is primarily observed during the summer, though autumn dust events can occur (Dagsson-Waldhauserova et al., 2015; Nakashima and Dagsson-Waldhauserová, 2019).

Dyngjusandur has distinct upwind, central, and downwind sections

and covers approximately 270 km^2 (parts were covered by lava during the 2014–2015 Holuhraun eruption; Pedersen et al., 2017) with a thickness of up to 10 m (Mountney and Russell, 2004). The bioaerosol sampling was conducted in the downwind region (Fig. 1; 64.97165°N, 16.57135°W), a flat, plane-bedded, and poorly sorted area composed volcanic glass, tephra, and lithic fragments (Baratoux et al., 2011). The rationale for sampling in this location was to capture the aerosols emitted from the central and upwind regions of the sandsheet. However, some bioaerosol emission might have been missed due to dust being lofted higher in the atmosphere prior to reaching the samplers.

2.2. Sampling and processing

Field campaigns occurred in July and August of 2022 and 2023. A field laboratory was established at the Dreki campsite (Fig. 1) and included a laminar flow hood with ultraviolet (UV) sterilization (Azzota Scientific) and a portable incubator (ReptiPro). Bioaerosol samples were collected via impaction onto quartz membrane filters (Pall Corporation) using the Deployable Particulate Sampler (SKC, Inc.) with a PM10 selective inlet mounted 1.5 m above the ground to avoid dust mobilization in the immediate vicinity of the sampler (Bottos et al., 2014). Quartz filters were sterilized (30 min UV on each side, 500 °C for 8 h; Dommergue et al., 2019) and inserted into the ethanol (EtOH) and UV-sterilized sampling apparatus aseptically. Filters inserted but not exposed to airflow were used as negative controls. Samples were collected for 24 h and up to 72 h at 15 L/min. In 2023, a higher volume aerosol sampler (SASS 3100, Research International, Inc.) was used at 300 L/min for 24 h (Mbareche Hamza et al., 2018). Filters were folded in half, flash-frozen in liquid nitrogen in the field, and then stored at −80 °C. Alternatively, filters were incubated in 1 mL 4% paraformaldehyde (PFA) for 1 h in the field followed by gentle suction to remove the liquid and then stored at −20 °C for later analysis with laser

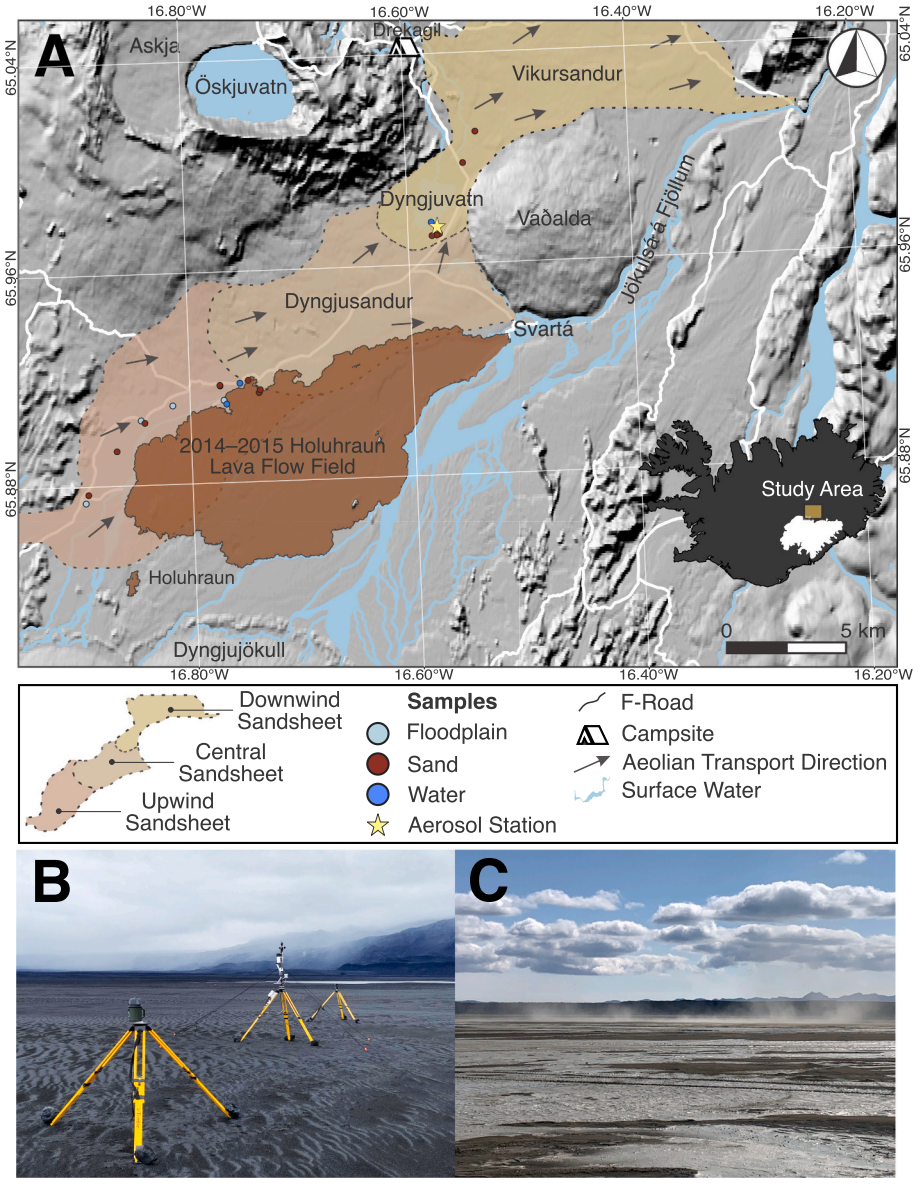

Fig. 1. Overview map and environmental context of the study area. (A) Dyngjusandur sandsheet within the Icelandic highlands. Sample site locations are indicated by the colored dots. Samples collected directly from glacial outflow are located further to the south at Kverkjöll and out of view of the map. The location of the aerosol samplers and weather station is indicated by the star located at the boundary of the central and downwind areas of the sandsheet. Basemap digital elevation model is from LANDSAT (NASA, USGS). Characterization of the sandsheet is modified from Mountney and Russell (2004) and Hudziak et al. (2025). (B) Photo of the aerosol samplers and weather station taken in 2023 (Credit: N. Hadland). (C) Photo of dust lofting at a dry diurnal floodplain in the morning near the margin of the 2014–2015 Holuhraun lava flow field (Credit: N. Hadland).

scanning microscopy.

To characterize source environments, sand (composed of basaltic fragments, eroded hyaloclastite, volcanic glass, and tephra), diurnal floodplain sediment, and water sources were collected from upwind, central, and downwind regions of Dyngjusandur, surrounding glacial outflows, and ponded water and lakes (Fig. 1). Sand and floodplain samples were collected aseptically by scraping the surface into 15 mL polypropylene tubes. Up to 665 mL (due to clogging filters) of water were filtered (Supplementary Material Table S1) onto Sterivex. All samples were flash-frozen in liquid nitrogen in the field. In total, we analyzed 12 bioaerosol, 17 sand, 8 diurnal floodplain, and 5 freshwater samples across the 2022 and 2023 field campaigns (Supplementary Material Table S1). Sampling and export were conducted under permits from the Icelandic Institute of Natural History and Vatnajökull National Park.

2.3. Weather data

We used high-resolution, site-specific weather data to investigate dispersal patterns, and to establish direct connections between local surface microbiota and airborne communities. To capture microclimate data during the bioaerosol samplings, weather data were collected at 30-s intervals using a HOBO U30 weather station (Onset Computer Corporation) co-located with the bioaerosol samplers, with sensors mounted on a telescoping tripod mast up to 4 m above the ground (Fig. 1b). Parameters included air temperature, relative humidity, rainfall, solar flux, barometric pressure, and wind speed and direction. Wind speed was recorded as the mean over logging interval whereas gust speed was defined as the highest 3-s gust. Wind direction was calibrated to true north (±5°). The mean wind direction ($\bar{\theta}$) was computed for each sampling period (e.g., 24 h) by vector averaging the angles θ_i in radians:

$$\bar{\theta} = tan^{-1}\left(\frac{\Sigma\, sin(\theta_i)}{\Sigma\, cos(\theta_i)}\right) \quad (1)$$

with an additional weighted version using wind speed scaled components. Total rainfall (mm) was summed over the period, and mean, minimum, maximum, and inter-quartile range (25th–75th percentiles) were calculated for all other parameters. Long-term seasonal data were obtained from the Upptyppingar station (65.06065°N, 16.21040°W) operated by the Icelandic Meteorological Office.

2.4. Culturing

To test the presence of culturable microorganisms, and to directly assess whether transported microorganisms remain viable in this harsh atmospheric environment, we used the drop plate method (Azua-Bustos et al., 2019). Sterile nutrient rich (Tryptic Soy Broth; TSB) and nutrient poor (R2A) agar plates were exposed on the ground for 24 h at the bioaerosol sampling site to trap airborne particles and saltating sand. Plates were then aseptically sealed and incubated at 11 °C (average ambient temperature) for up to 2 weeks in the field. Single colonies were re-streaked three times for purity, grown again in nutrient broth, and preserved in 25% glycerol at −80 °C. Sand and floodplain samples were also cultured by adding ~5 g of sample to the broth. DNA was extracted using the DNeasy Biofilm DNA Extraction Kit (Qiagen) and then the 16S ribosomal RNA (rRNA) was amplified using primers F9 and R1544R and primer R805 internal of the 16S rRNA gene for Sanger sequencing on an Applied Biosystems 3730XL DNA Analyzer. Sequences were edited, classified, and identified through BLAST searches in GenBank. GenBank accession numbers are PV624792–PV624803.

2.5. Microscopy

To visualize associations between microbial cells and dust particles that may enhance atmospheric survival, PFA fixed filters were submerged in 30% EtOH and 70% (1×) Phosphate Buffered Solution (PBS). The tube was placed in an ice slurry (to prevent overheating) and the probe of a Branson digital sonifier 150 was positioned 1 cm away from the sample to detach the grains from the filter while limiting microbial removal from grains. The following settings were used: pulse, timed, 40% amplitude, 30 s on, 1 min off, 3 min on in total, as a variation of previously described methods (Duhamel and Jacquet, 2006). The rinsate was then filtered onto 0.1 μm grey polycarbonate (PCTE) filter. The sonication steps were repeated on the same sample soaked in fresh EtOH:PBS (1:1) and filtered through the same PCTE filter (to collect and concentrate further grains). The PCTE filter was then rinsed 3 times with 1× PBS, for 5 min each, discarding the effluent flowing through the filter. Filters were stained directly with 4000:1 SYBR Gold (Invitrogen) dilution in 1× PBS, incubated in the dark for 20 min, rinsed with 1× PBS twice, followed by 50%, 80%, and 90% EtOH washes, incubating 5 min each wash. Half of the filter was placed onto a clean glass slide, mounted with Citifluor™—Antifadent Mountant Solutions (Electron Microscopy Science), covered with a coverslip, and stored overnight at −20 °C.

Filter halves were imaged using a laser scanning confocal microscope (Leica Stellaris 5 on a DMI8 microscope), equipped with a white light laser and its unique fluorescence lifetime based TauSense® technology. A low magnification overview map was created to identify promising regions of higher particle density and subsequent higher resolution microscopy areas were identified using a nested dataset approach (Neveu et al., 2018). Additionally, 15 random fields of view were captured for cell counts. The samples were excited at 496 nm and emitted light collected in the emission window 525–615 nm, capturing emission maxima at around ~540 nm of SYBR gold. Finally, a Tau lifetime scan was collected at each imaged grain to assess the presence of mineral autofluorescence. Excitation at 405 nm (emission 415–485 nm) and at 663 nm (emission 675–825 nm) were employed to evaluate potential UV-generated autofluorescence from grains and the presence of chlorophyll-harboring microbes, respectively. Stained biomass was located and logged using the "Cell Counter" plugin (Kurt De Vos, Univ Sheffield, Academic Neurology, https://imagej.net/ij/plugins/cell-counter.html) in ImageJ/FIJI. However, microbes removed during processing or located on the filter side of optically opaque grains would not be enumerated. Moreover, biofilms are agglomerations of cells, obfuscating absolute enumeration. The reported values therefore should be considered minimums.

2.6. DNA extractions

Due to the low biomass nature of bioaerosol samples, enhanced precautions were employed during sample handling, including working in a specified environment for molecular biology work and in a PCR clean hood (AirClean Systems), personnel masking, and working on EtOH and bleach sterilized surfaces. DNA was extracted using a modified DNeasy PowerWater Kit (Qiagen) method (Basapathi Raghavendra et al., 2023; Dommergue et al., 2019). Briefly, cylindrically rolled filters were placed into a preheated (60 °C) lysis buffer, sonicated at 45 KHz at 65 °C for 30 min, and homogenized using a FastPrep-24 (MP) bead beater (45 s at 6.5 m/s × 2), placing the tubes on ice between runs. Lysates were recovered by centrifugation (1000 *g*, 4 min) through a sterile syringe inserted into a 50 mL tube to prevent excessive absorption of liquid by filter debris (Dommergue et al., 2019), then purified and eluted following the manufacturer's instructions. DNA from sand and floodplain samples was extracted using the DNeasy PowerSoil Pro Kit (Qiagen), with extraction blanks consisting of unused bead tubes processed alongside samples. DNA from water samples was extracted using the DNeasy PowerWater Sterivex Kit (Qiagen), with extraction blanks consisting of unused Sterivex filters. DNA concentrations were quantified using a Qubit Fluorometer (Thermo Fisher Scientific) with the high-sensitivity dsDNA assay.

2.7. Sequencing and data processing

To identify prokaryotic and eukaryotic taxa in atmospheric and source samples and enable quantitative community comparisons, the 16S rRNA gene (v4 region) and 18S rRNA gene (v9 region) were amplified using primers 515F/806R and Euk1391/eukbr respectively, with 35-cycle PCR (95 °C 5 min; 35 cycles of 95 °C 30 s, 53 °C 40 s, 72 °C 1 min; final elongation 72 °C 10 min) using HotStarTaq Plus Master Mix Kit (Qiagen). PCR products were checked in a 2% agarose gel, multiplexed using unique dual indices, and then pooled in equal proportions based on molecular weight and DNA concentration. The pooled samples were purified using calibrated Ampure XP beads and sequenced at MR DNA (Shallowater, TX, USA) on an Illumina MiSeq.

Raw sequences were processed in QIIME2's Python API (v2024.10; Bolyen et al., 2019). Demultiplexing and primer removal were performed using Cutadapt (Martin, 2011). Denoising, chimera removal, and forward and reverse read merging were completed using DADA2 (Callahan et al., 2016). Taxonomy assignment used a custom SILVA database (v138.1; Yilmaz et al., 2014) built using RESCRIPt (Robeson II et al., 2021). Representative sequences for each amplicon sequence variant (ASV) were used for taxonomic assignment using the built database. A phylogenetic tree was created using MAFFT alignment (Katoh et al., 2002) and FastTree (Price et al., 2009). Metabolic functional interferences were conducted using FAPROTAX, which maps ASVs to broad ecological functions based on implicit assignments of a trait to taxa (Louca et al., 2016), and PICRUSt2 (Douglas et al., 2020), which uses genome reconstruction to predict MetaCyc pathway abundances. Pathway inferences were normalized to per-sample relative abundances. The rationale for including these pipelines was to capture complementary perspectives on microbial function variation. Results must be interpreted with caution since FAPROTAX assumes functional uniformity within taxa, while PICRUSt2 relies on reference genomes.

Cross-contamination due to 'tag switching,' or barcode sequencing errors (cross-talk) is enhanced in low biomass samples (Eisenhofer et al., 2019). Sequences matching *Staphylococcus, Finegoldia, Lactobacillus, Bradyrhizobium,* and *Streptococcus* in the 16S dataset were removed based on abundances in blanks. These taxa, though found in bioaerosols, are common contaminants (Eisenhofer et al., 2019). Additional filtering used the decontam package (Davis et al., 2018), removing features with $p < 0.1$. This approach identifies contaminants based on their prevalence in true samples versus controls and performs well with low biomass samples (Karstens et al., 2019). A summary of contaminants removed is shown in Supplementary Material Fig. S1. Mitochondrial and chloroplast sequences found in the 16S dataset and prokaryotic sequences found in the 18S dataset were removed from the analyses. After processing, the minimum sequencing depth was 43,050, which was used as the rarefaction depth in statistical analyses. Sequencing data are available in the GenBank (accession numbers: SAMN48399260–SAMN48399309, BioProject: PRJNA1260575).

2.8. Statistical analyses

To assess relationships between environmental conditions and microbial community structure, and to quantitatively attribute bioaerosol sources, we employed multiple complementary statistical approaches. Alpha diversity using Faith's phylogenetic diversity (PD) and Shannon's index, and beta diversity using weighted Unifrac (Lozupone and Knight, 2005) and Jaccard distances were analyzed using QIIME2. Faith's PD incorporates the lengths of branches on the phylogenetic tree while Shannon's index incorporates richness (number of species) and evenness (relative abundance of species). Weighted Unifrac incorporates phylogenetic distances and taxon abundance, whereas Jaccard uses presence/absence only. Beta diversity correlations with environmental variables were assessed via Mantel tests (QIIME2's diversity beta-correlation). Briefly, a distance matrix for each weather parameter was constructed to quantify pairwise differences in environmental conditions. Spearman's correlation (ρ) was computed, and statistical significance was assessed using 999 permutations by permuting one matrix to obtain a null distribution.

Relationships between alpha diversity and meteorological variables were assessed using linear fixed-effects models incorporating weather parameters as explanatory variables. Sampling volume (the total air volume collected) differed between samples and therefore needed to be accounted for in downstream statistical analyses. Sampling volume was treated as a fixed effect to control the variability introduced by differences in air sampling duration and instrument used across samples, ensuring alpha diversity estimates were not confounded by sampling. The linear fixed effects model was conducted using the Python package pymer4 (Jolly, 2018) to generate a slope and y-intercept, where individual meteorological parameters were tested separately. Pairwise Kruskal–Wallis tests were conducted for wind speed weighted wind directions binned into NE, NW, SE, SW quadrants to test the effect of wind direction on alpha diversity.

To determine the impact of environmental filtering on microbial community structure, phylogenetic null modelling was used to test if phylogenetic distribution was more or less clustered than expected by chance (Stegen et al., 2012). Phylogenetic clustering typically occurs when environmental conditions select species that have similar traits. Conversely, phylogenetic overdispersion occurs due to competitive exclusion. The trans_nullmodel class in the microeco R package (Liu et al., 2021) was used with the metrics net relatedness index (NRI) and the nearest taxon index (NTI). NRI is calculated as the mean pairwise phylogenetic distance of taxa in a single sample:

$$NRI = -\frac{mn(X_{obs}) - mnX(n)}{sdX(n)} \tag{2}$$

where X_{obs} is the phylogenetic distance between two taxa, $mn(X_{obs})$ is the pairwise mean distance of all (n) taxa, and $mnX(n)$ and $sdX(n)$ are the mean and standard deviation, respectively, based on a null model consisting of shuffling the tree branches in the sample pool over 10,000 iterations. Similarly, NTI is a measure of phylogenetic distance to the nearest taxon on the tree:

$$NTI = -\frac{mn(Y_{obs}) - mnY(n)}{sdY(n)} \tag{3}$$

where Y_{obs} is the phylogenetic distance to the nearest taxon, $mn(Y_{obs})$ is the observed mean nearest taxon distance, and the other parameters are calculated as in Eq. 2 (Webb et al., 2002). NRI therefore describes phylogenetic structure across all possible pairs of taxa in a community, while NTI captures fine-scale clustering.

To quantitatively determine the contribution of different terrestrial sources to the airborne community, microbial source attribution to bioaerosols was performed using the Bayesian algorithm SourceTracker2 on rarefied data (Knights et al., 2011), assigning proportions of sequences from sand, diurnal floodplain sediment, and water sources. SourceTracker2 probabilistically estimates the proportional contribution of each source environment to the sink (bioaerosol) community, without assuming complete preservation of source communities during transfer. The algorithm includes an "unknown" category that captures sequences in the sink that cannot be confidently attributed to any characterized source environment, accounting for unsampled source environments, or novel taxa in the atmosphere.

Pairwise comparisons in beta diversity between sources and bioaerosols were conducted using Permanova tests with 999 permutations to generate a null distribution. Overlapping ASVs across sample types were determined using microeco (Liu et al., 2021).

2.9. HYSPLIT trajectories

To assess the potential for long-range microbial transport and identify possible pathways for bioaerosol dispersal to population centers,

dust transport from Dyngjusandur was analyzed using forward trajectory modelling through the Hybrid Single-Particle Lagrangian Integrated Trajectory (HYSPLIT) tool (Stein et al., 2015). HYSPLIT computes the position of an air parcel carried from a starting position as driven by three-dimensional winds. These trajectories demonstrate *potential* pathways of dust, rather than direct dust emissions (Baddock et al., 2017). Consequently, not all the modeled trajectories necessarily contain suspended dust. Five-day forward trajectories were initiated at 100 m above ground level starting at each hour during the study periods in 2022 and 2023, using the GDAS database (Baddock et al., 2017). We select this height, which is lower than typical for HYSPLIT, to maximize the possibility that trajectories contained dust and potentially bioaerosols, rather than an estimation of the longest possible range. Additionally, shorter or longer residence times are possible for bioaerosols (Mayol et al., 2017), but HYSPLIT's accuracy decreases over longer timescales. Five-day backwards trajectories were also conducted to determine the possible origin of distinct microbial populations. Models were executed in Python using the PySPLIT package (Warner, 2018). Trajectories were clustered using HYSPLIT's variance-based algorithm to group similar paths and summarize patterns. Dust emission during the study periods was corroborated using Atmospheric Infrared Sounder (AIRS) dust scores obtained from NASA Worldview. Dust scores exceeding 380, indicating probable dust presence, were observed over central Iceland on seven days during the 2022 campaign (July 19, 22, 26; August 3, 4, 5, 6) and three days during the 2023 campaign (July 29, 30; August 5). AIRS dust detection is optimized for bright mineral dust and may underestimate dark basaltic dust from Icelandic sources; consequently, dust emission likely occurred on additional days not captured by satellite observations.

2.10. Particle size analysis

To characterize the grain size distributions of potential source sediments, particle size distributions of sand and diurnal floodplain samples were measured in triplicate using a laser diffraction particle size analyzer (Microtrac) equipped with a recirculating pump and internal ultrasonic dispersion capabilities at Particle Size Labs LLC. Samples were dry sieved, if necessary, through a 2000 μm mesh to remove coarse material, homogenized, and then added to the instrument's recirculation chamber filled with deionized water. The instrument's internal ultrasonic probe was activated 30 s prior to each measurement. Analysis parameters included volcanic sand optical properties (refractive index = 1.60, transparent, irregular shape) appropriate for basaltic materials. Measurements were conducted with 4 rinse cycles and three replicate 30 s runs averaged for each sample. Data processing was performed using Microtrac FLEX software (v12.1.2), which calculated volume-weighted distribution parameters including mean diameter (MV), median diameter (D50), and percentile values.

2.11. Sediment transport calculations

To determine which particle sizes could be mobilized under observed wind conditions during bioaerosol sampling periods and thereby constrain the physical mechanisms of microbial entrainment, we implemented Melosh (2011)'s discussion of sediment transport, using a threshold calculation where the drag force exceeds the gravitational force. Under the assumption that grains protrude above the viscous sublayer—where turbulence is suppressed next to the surface—each grain is subjected to a drag force proportional to the shear stress times surface area. This is resisted by the effective weight of the grain (its weight reduced by air buoyancy). Equating these forces and solving for the friction velocity (v_*), a measure of wind shear stress, yields:

$$v_* = \mathrm{A}\sqrt{\frac{gd(\rho_s - \rho_a)}{\rho_a}} \tag{4}$$

where d is the grain size, ρ_a is air density, ρ_s is grain (basalt) density, and A is an empirical coefficient taken here as 0.1 (Melosh, 2011). In reality, A varies with grain geometry, soil moisture and cohesion, electrostatic forces, and van der Waals forces, especially at small grain sizes, where higher wind speeds are required to transport sediment. Moreover, larger particles undergo saltation rather than sustained suspension, and upon impact can eject finer particles. However, detailed modelling and empirical measurements of these effects are beyond this study's scope (Field and Pelletier, 2018). We then calculate the threshold wind velocity at height z using:

$$v(z)_t = 5.75 v_* \log\left(\frac{z}{z_0}\right) \tag{5}$$

where $z_0 = 1$ mm represents the roughness factor, based on ripple heights of a few cm at Dyngjusandur (Mountney and Russell, 2004). Using 30 s wind speeds measured at $z = 4$ m, we compute, for each bioaerosol sample, the fraction of the sampling period during which wind exceeded the threshold across a range of grain sizes.

3. Results

3.1. Meteorological conditions shape airborne microbial diversity and community structure

The 2022 and 2023 field campaigns captured a broad range of meteorological conditions, providing an opportunity to assess how weather variability influences airborne microbial communities (Supplementary Material, Fig. S2). For example, a low-pressure system during the 2022 sampling campaign resulted in sustained winds exceeding 16 m/s, while 2023 was comparatively calmer, with gusts rarely exceeding 8 m/s.

After accounting for sampling volume, there were statistically significant relationships of alpha diversity (Faith's PD and Shannon's index) with weather variables for the bioaerosols, a selection of which are shown in Table 1. Temperature, wind speed, and gust speed had significant ($p < 0.05$) or moderately significant ($p < 0.1$) positive relationships with alpha diversity. Pressure (mean, minimum and lower quartile) had a negative relationship with alpha diversity. In other words, low pressure storm systems resulted in a higher Shannon's index. 18S metrics had similar relationships, except for temperature. Other weather measures and statistics (e.g., mean and maximum wind speed) for alpha diversity indices were found to be significant or moderately significant but not included in the table for simplicity (see Supplementary Material Table S2). A pairwise Kruskal–Wallis test for both Faith's PD and Shannon's index did not result in significant differences with respect to wind speed weighted wind directions binned into NE, NW, SE, SW (Supplementary Material Table S3). The 18S Shannon diversity pairwise comparison between NE and SW bins was moderately significant ($p = 0.064$).

NRI and NTI analyses revealed values greater than zero for both 16S and 18S datasets (Fig. 2) due to phylogenetic clustering, which is typically a result of environmental filtering (Stegen et al., 2012). Linear fixed effects models applied to NRI and NTI values against environmental variables found significantly positive relationships with maximum gust speed and wind speed for NTI (Supplementary Material Table S2), like the relationships with alpha diversity.

Mantel tests were used to evaluate the correlation between weather variables and beta diversity to assess shifts in bioaerosol community composition. To determine whether sampling volume influenced the trends, the test was conducted on a distance matrix based on sampling volume. No significant relationships were found for both 16S and 18S datasets (Supplementary Material Table S4), suggesting that variations in sampling volume did not introduce systematic biases in community composition. The Mantel test was then applied to weather variables, and certain significant relationships are reported in Table 2. A positive

Table 1
Linear fixed effects models of alpha diversity indices with respect to select weather parameters.

	16S						18S					
	Faith's PD[a]			Shannon			Faith's PD			Shannon		
Var[b]	*m*[c]	*SE*[d]	*p-value*	*m*	*SE*	p-*value*	*m*	*SE*	p-*value*	*m*	*SE*	p-*value*
T_{max}[f]	4.86	2.32	0.07	0.44	0.23	0.09	n.s.[e]	n.s.	n.s.	n.s.	n.s.	n.s.
GS_{Q3}[g]	7.48	4.06	0.10	0.73	0.38	0.09	6.47	3.49	0.10	0.70	0.31	0.05
WS_{Q3}[h]	n.s.	n.s.	n.s.	0.76	0.41	0.09	n.s.	n.s.	n.s.	0.72	0.33	0.06
P_{min}[i]	n.s.	n.s.	n.s.	−0.27	0.11	0.03	n.s.	n.s.	n.s.	−0.25	0.08	0.01

[a] Faith's Phylogenetic Diversity (PD).
[b] var = weather variable.
[c] m = slope.
[d] SE = Standard Error.
[e] n.s. = not significant.
[f] T = Temperature.
[g] GS = Gust Speed.
[h] WS = Wind speed.
[i] P = Pressure.
max = maximum value.
Q3 = upper quartile.
min = minimum value.

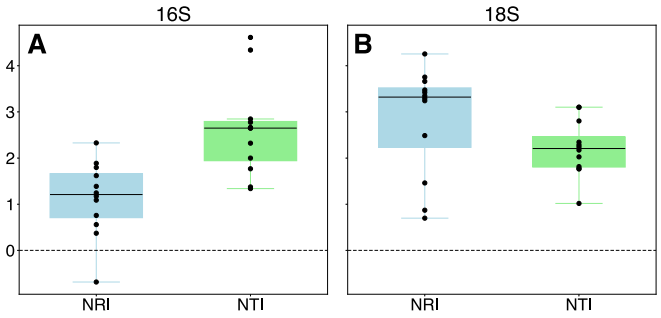

Fig. 2. Box and whisker plots of Net Relatedness Index (NRI) and Nearest Taxon Index (NTI). Separate plots are shown for (A) 16S and (B) 18S datasets. The horizontal dashed line at zero denotes the transition from phylogenetic clustering (NRI or NTI > 0), associated with strong environmental filtering, to phylogenetic overdispersion (NRI or NTI < 0), associated with competitive exclusion.

Spearman's ρ suggests that as differences in each weather parameter between sample pairs increase, so do differences in microbial community structure. Gust speed was significantly correlated with weighted Unifrac distances ($p = 0.032$), while wind speed showed a similar positive trend ($p = 0.065$; Table 2). Pressure variables were similarly significantly correlated with Jaccard distances (Table 2; Supplementary Material Table S4). Pairwise permanova tests for both weighted Unifrac and Jaccard metrics did not have differences between wind speed weighted binned wind directions, like alpha diversity (Supplementary Material Table S5), except for pairwise comparisons between NW and SE for both Jaccard ($p = 0.079$) and weighted Unifrac ($p = 0.062$) for 18S data which were moderately ($p < 0.1$) significant.

3.2. Storm events enhance coupling between surface sources and atmospheric microbial communities

The Bayesian algorithm SourceTracker2 requires that each source has a distinct fingerprint. Sand, diurnal floodplain, and fluvial source environments harbored distinct microbial communities (Supplementary Material Fig. S3), with pairwise permanova tests confirming significant differences between all source categories (Supplementary Material Table S5). The model revealed that bioaerosols were sourced from a combination of all three categories—sand, diurnal floodplain, and freshwater. However, a large fraction came from an unknown source

Table 2
Mantel correlations between the distance matrices of beta diversity (Weighted Unifrac and Jaccard) and select weather parameters.

	16S				18S			
	Weighted Unifrac		Jaccard		Weighted Unifrac		Jaccard	
Var[a]	*ρ*[b]	p-*value*	*ρ*	p-*value*	*ρ*	p-*value*	*ρ*	p-*value*
GS_{Q3}[d]	0.301	0.032	[c]n.s.	n.s.	n.s.	n.s.	n.s.	n.s.
WS_{Q3}[e]	0.283	0.065	n.s.	n.s.	n.s.	n.s.	n.s.	n.s.
P_{Q1}[f]	n.s.	n.s.	0.388	0.008	n.s.	n.s.	0.326	0.053
RH_{max}[g]	n.s.	n.s.	n.s.	n.s.	n.s.	n.s.	0.318	0.076

[a] Var = weather variable.
[b] *ρ* = Spearman's rho.
[c] n.s. = not significant.
[d] GS = Gust Speed.
[e] WS = Wind Speed.
[f] P = Pressure.
[g] RH = Relative Humidity.
max = maximum value.
Q3 = upper quartile.
min = minimum value.

(Fig. 3). Two of the bioaerosol samples at lower wind speeds had no species attributable to the categorized source environments. Moreover, the lower wind speeds had a slightly higher proportion sourced from fluvial sources, up to 19.923 ± 0.006% (mean ± SD). Conversely, higher wind speeds had a higher contribution of sand and floodplain sediment, with the bioaerosol collected during the windiest day (collected in 2022) having 75.593 ± 0.015% sand as the inferred source of microorganisms. Below 8.56 m/s maximum gust speed, there was very little contribution of sand- (≤0.395 ± 0.003%) or floodplain-based (≤0.597 ± 0.006%) microorganisms to the bioaerosol samples.

Sediment transport modelling provided a mechanistic explanation for this threshold. Modeled emission patterns varied markedly across sampling periods, with calm conditions mobilizing only fine particles (<90 μm) while storms exceeded threshold velocities for sand-sized grains (>400 μm; Fig. 4). Particle size analysis additionally revealed that the sand was substantially coarser (volume-weighted mean diameters of 426–456 μm) than diurnal floodplain deposits (~82 μm;

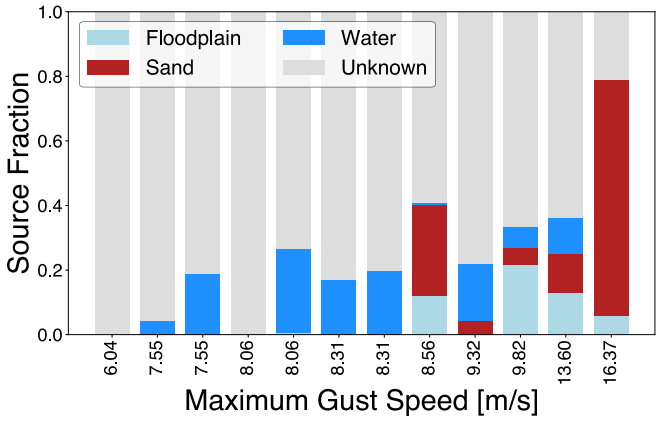

Fig. 3. Quantitative source tracking of microorganisms sourcing the bioaerosols using a Bayesian model. Each color represents the mean fractional contributions of each source (sand, diurnal floodplain, and freshwater) to each sink (bioaerosol), with each bar representing a unique sample on different days.

Supplementary Material Fig. S4), consistent with the higher wind speeds required to mobilize sand-associated microorganisms observed in the source tracking analysis.

Aerosols had several distinct ASVs (1714) when compared to surface source environments, but 121 were common between the aerosols and all three sources (Supplementary Material Fig. S5). The greatest overlap with aerosols was observed for the sand environments, which shared 337 ASVs with aerosols, compared to 43 shared with floodplain alone, and 109 with water alone. The top groups that were present in all environments at the family level were Beijerinckiaceae, Methylophilaceae, Solirubrobacteraceae, Comamonadaceae, Pseudanabaenaceae, Gemmatimonadaceae, Chtinophagaceae. Specific genera in these groups included *Methylotenera*, *Conexibacter*, *Polaromonas*, *Pseudanabaena, Gemmatimonas*, and *Rhizobacter*.

Comparing beta diversity of the categories also provided useful qualitative insight into the coupling of bioaerosols and source environments (Fig. 5). For weighted Unifrac, bioaerosols generally grouped separately from the sand, diurnal floodplain, or fluvial sources, but samples with higher wind speeds and lower pressures (e.g., more extreme weather events, <930 mbar) were more closely associated with the sand and floodplain, corroborating the SourceTracker2 analysis. One fluvial source from ponded water in the diurnal lake region of the sandsheet clustered closely with the aerosols. Similar associations are shown in a PCoA of the Jaccard metric—most of the bioaerosols were distinct with a close association of the ponded water sample as well as glacial outflow (Fig. 5b). Pairwise permanova tests for both Unifrac and Jaccard metrics showed significant differences ($p < 0.05$) between source environments and bioaerosols, except for the freshwater–bioaerosols comparison with the Jaccard metric, which was only moderately significant (Supplementary Material Table S5; $p = 0.082$). Pairwise Kruskal–Wallis tests revealed significant or moderately significant differences in Faith's PD and Shannon's diversity between bioaerosols and source environments (Supplementary Material Table S3), except for the fluvial—bioaerosol comparison for Shannon diversity ($p = 0.46$).

3.3. Particle attachment and viability of airborne microorganisms

Source tracking analyses indicated that microorganisms from the sandsheet enter the atmosphere during storm events but did not address whether they survived transport or remained associated with particles. We addressed this through complementary culture-based and microscopy approaches. Airborne and sand-associated microorganisms were isolated from both nutrient rich (TSB) and nutrient poor (R2A) media to assess the presence of viable cells capable of surviving environmental exposure and transport (Supplementary Material Table S6). Six bacterial species were successfully cultured from sand and aerosol drop plate samples, confirming the viability of microorganisms associated with the sandsheet and its emissions. The isolates included potentially cold-adapted taxa such as *Pseudomonas antarctica*, *Arthrobacter* sp., and *Pyschrobacter* sp. which have been isolated from polar and cryospheric environments, such as Iceland (Daussin et al., 2024; Kelly et al., 2014). *Pseudomonas syringae*, a known ice-nucleating species that can act as cloud condensation nuclei (de Araujo et al., 2019), was recovered from a sandsheet sample. Moreover, this species along with members of *Arthobacter* can be opportunistic pathogens of crops (Hirano and Upper,

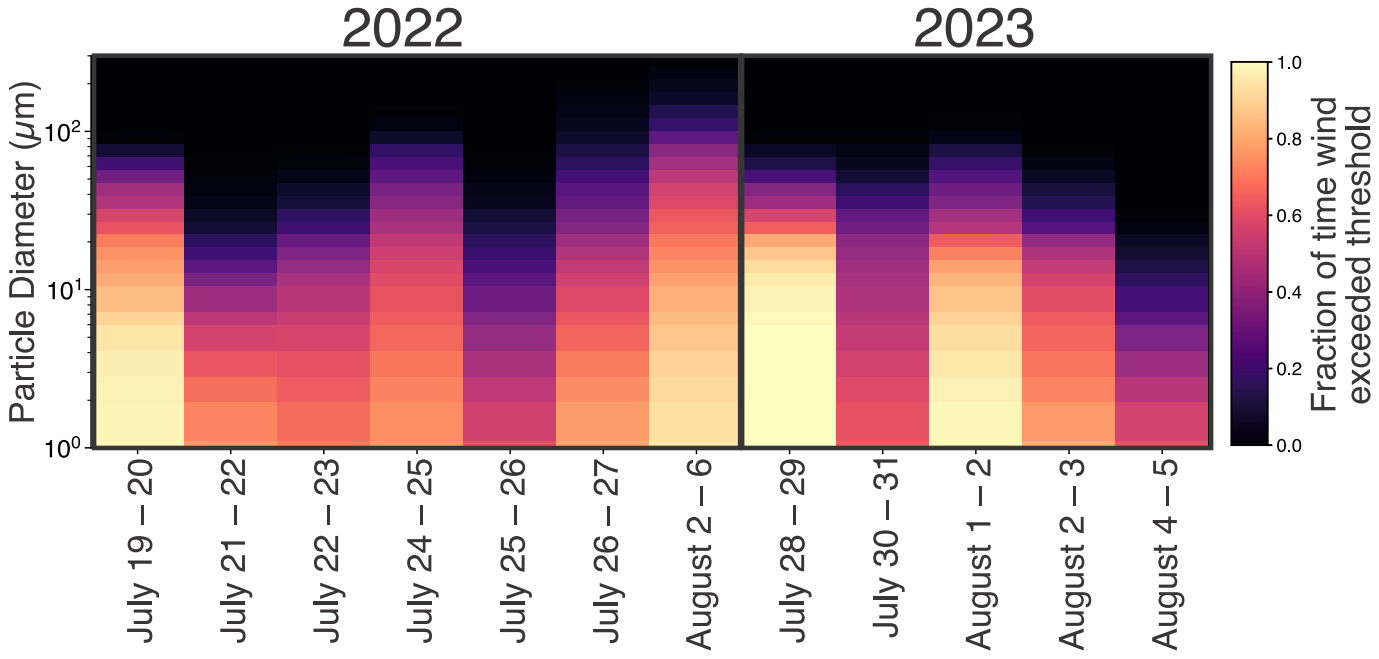

Fig. 4. Sediment transport model. Fraction of time during the sampling window that the wind speed exceeded a threshold where the drag force overcomes the force due to gravity.

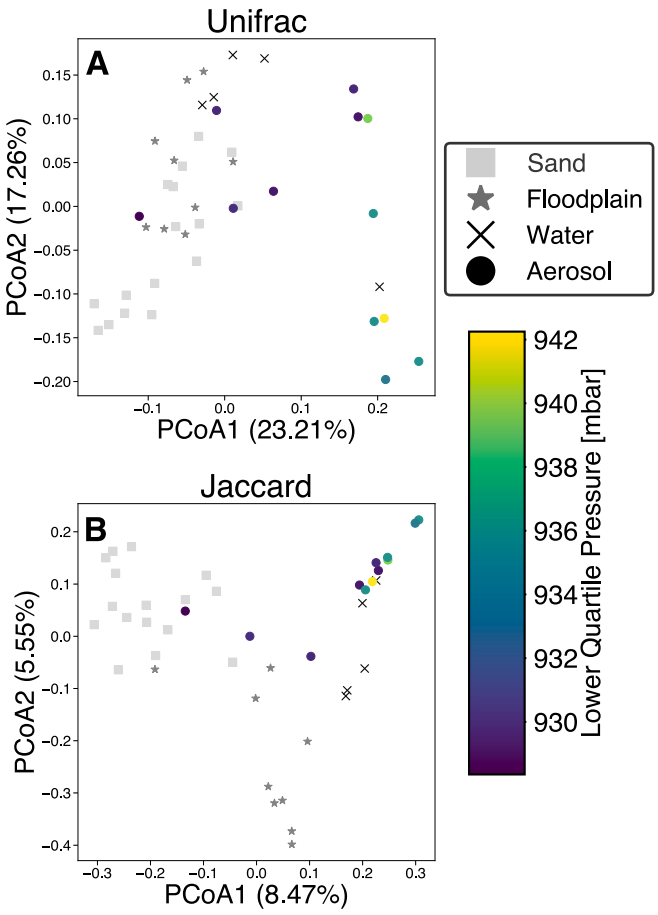

Fig. 5. Principal Coordinate Analyses (PCoA) of beta diversity. PCoA's are conducted using the distance matrices of (A) the weighted Unifrac and (B) Jaccard metrics. The variation explained for individual principal coordinates are listed on the axis legends. Aerosol samples are colored according to the lower quartile pressure during the sampling period.

2000).

To determine whether these viable taxa were transported in association with dust particles, we examined aerosol filter samples using confocal laser scanning microscopy (Fig. 6). After checking for mineralogical autofluorescence (Supplementary Material Fig. S6), laser scanning confocal microscopy revealed the presence of individual cells and biofilm-like structures coating dust particles captured as aerosols on a relatively calm day in 2023 (mean wind speed = 1.87 m/s). Two visually distinct types of particles were observed: (1) darker, optically opaque, and topographically complex grains (Fig. 6a–c), and (2) lighter-toned, largely transparent, and smoother grains (Fig. 6d–f). Cell counts from random fields of view, based on nucleic acid staining with SYBR Gold, were significantly higher on the darker, rougher grains (165 ± 107 cells; mean ± SD), than the smoother, lighter particles (73 ± 37; Kruskal–Wallis, $p = 0.045$; Supplementary Material Fig. S7). When both particle types were in close spatial proximity (Fig. 6g–i), cellular biomass was predominantly associated with the more topographically complex and darker surfaces. Chlorophyll fluorescence, indicating the presence of photosynthetic organisms, was rarely observed (Supplementary Material Fig. S6).

3.4. Bioaerosols contain distinct taxa with potential for long-range transport

The microbial diversity in the aerosol samples, based on 16S rRNA gene sequencing, was dominated by Actinobacteria, Gammaproteobacteria, Alphaproteobacteria, Bacilli, Bacterioida, and Thermoleophilia at the taxonomic level of class (Supplementary Material Fig. S8). There were also 12 families belonging to Cyanobacteriota, up to 6.2% relative abundance (for Nostocaceae, specifically *Anabaena* sp.). Additionally, several samples had ASVs—up to 14.5%—that could not be assigned to a known phylum, suggesting the presence of novel or poorly characterized microbial lineages in this environment. Several ecologically relevant bacterial genera were identified. For instance, *Actinetobacter* and *Cupriavidus,* which can grow on nutrients leached from basalt (Byloos et al., 2018), *Paeniglutamicibacter,* which has been cultivated from different cold environments, including Antarctica (Busse, 2016), and *Sphingomonas* previously isolated from the atmosphere and young lava rocks in Iceland (Daussin et al., 2023). While we detected *Corynebacterium*, a genus identified in a number of environmental soil samples and known to include potential human pathogens, we note that it has also been reported as a DNA extraction contaminant (Eisenhofer et al., 2019). However, its presence in only one laboratory blank sample suggests that most detections represent genuine environmental occurrences rather than systematic contamination, with the single blank detection potentially attributable to tag switching during sequencing. The FAPROTAX metabolic interference pipeline revealed that chemoheterotrophy dominated across all bioaerosol samples, while nitrate reduction, fermentation, aromatic compound degradation, phototrophy, and some pathogen-associated functions were also present (Supplementary Material Fig. S9a). Nitrogen cycling (ureolysis, ammonia oxidation, and nitrification) and C1 metabolisms (methanol oxidation and methylotrophy) had statistically significant ($p < 0.05$) increases in relative abundance under lower atmospheric pressures, or stormy conditions (Supplementary Material Fig. S9b). Complementary PICRUSt2 analysis predicted that peptidoglycan maturation and fatty-acid salvage (e.g., cell envelope remodeling) were the most abundant pathways, while phytol degradation signaled microbial use of plant/algal material (Supplementary Material Fig. S10). These predictions should be interpreted with caution however, as they rely on 16S rRNA amplicon sequencing. As such, the analysis is exploratory and intended to serve as a hypothesis-generating tool for identifying potential functional shifts.

Eukaryotes in the bioaerosol samples identified using the 18S rRNA gene included fungi, algae, protists, and plants (Supplementary Fig. S8). Specifically, top fungal classes included Agaricomycetes, Dothideomycetes, and Leotiomycetes. One of the most abundant (up to 30% relative abundance) belonged to the order Agaricales, an extremely diverse group, also found previously in Iceland (Gulden and Hallgrimsson, 2000). Major fungal genera identified were *Amylocorticium*, *Helotiales*, *Cladosporium*, and *Ascochyta,* all of which are involved in plant decay and can be pathogenic to crops. The major protist group identified was the unicellular spore forming parasite Apicomplexa. Sarcomonadea, Phyllopharyngea, and other protist classes were also present in small amounts. Major algal classes included members of Trebouxiophyceae, Ulvophyceae, and Chlorophyceae (specifically, the genus *Chlamydomonas*). The identified plant orders were Poales, Solanales, and other minor groups. Both the Solanales and Poales are species-rich and are ecologically and economically important (Elliott et al., 2024; Särkinen et al., 2013).

Forward trajectory modelling provided an estimate of the potential geographic reach of these bioaerosol taxa. Fig. 7 presents a comparison of clustered HYSPLIT trajectories run on an hourly basis for the bioaerosol sampling periods in 2022 and in 2023 (Baddock et al., 2017). Air masses emitted from the sandsheet reached several geographic areas in Europe, including the British Isles, Norway, Svalbard, and mainland Europe (e.g., France, Belgium, Denmark, and the Netherlands). A few trajectories also circulated within Iceland, reaching Reykjavík. For example, 31% of trajectories in 2022 and 40% in 2023 headed west towards Reykjavík, and some air masses continued towards Greenland. While there were more trajectories heading further south in 2023 compared to 2022, both years consistently reached major population

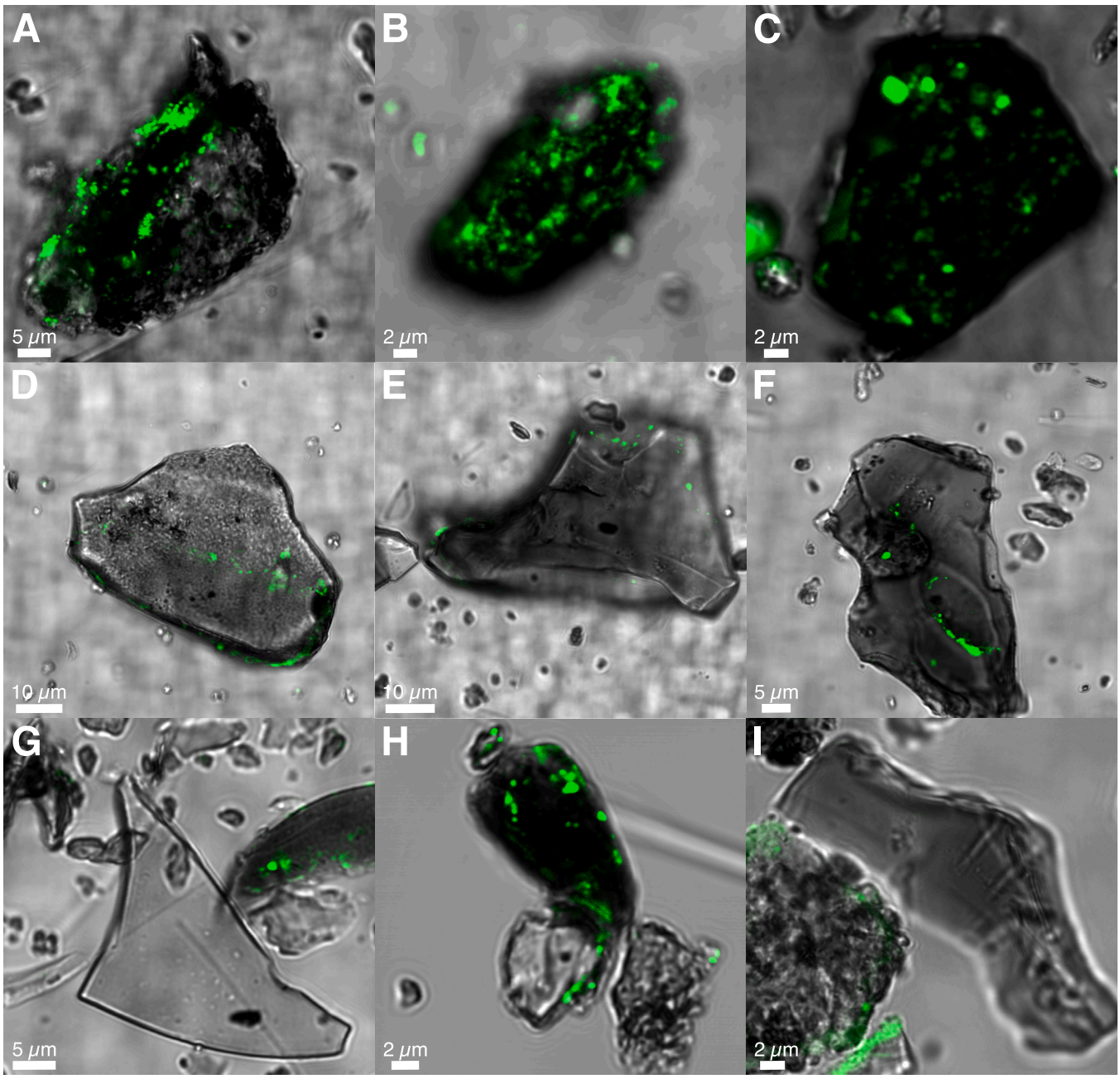

Fig. 6. Laser scanning confocal microscopy images of representative particles. Images show dark-toned (A–C), light-toned (D—F), and other (G–I) dust particles captured using an aerosol sampler. Green fluorescence indicates nucleic acid staining with SYBR Gold.

centers in mainland Europe and the British Isles. This modelling approach has inherent limitations due to a lack of constraints on dust emission and deposition processes. However, actual atmospheric residence times for microbe-carrying particles may exceed the 5-day simulation period presented here, particularly for finer particles that could remain suspended for extended periods (Mayol et al., 2017). Backwards trajectories show that most air parcels arriving at Dyngjusandur came from the North Atlantic and eastern Greenland. Some trajectories came from the south and west (e.g., from northern Canada; Supplementary Material Fig. S11).

4. Discussion

A central question in atmospheric microbiology is whether airborne microbial communities are assembled passively through stochastic aerosolization or actively shaped by environmental selection pressures (Lappan et al., 2024). In other words, there is a possibility of obligately atmospheric (e.g., never landing) microorganisms that may play underappreciated roles in global biogeochemical cycles (Fröhlich-Nowoisky et al., 2016). In this study, we found that bioaerosols at Dyngjusandur were compositionally distinct from, yet still partially traceable to local surface sources. Diversity and phylogenetic structure were strongly correlated with meteorological variables, particularly wind/gust speed and pressure, suggesting that extreme weather events act as environmental filters, selectively entraining microbes into the atmosphere and potentially enabling their transport to populated regions. The microbial community structure of the local atmosphere therefore is likely a reflection of surrounding surface environments, selective processes, meteorological variables, and possibly long-range transport.

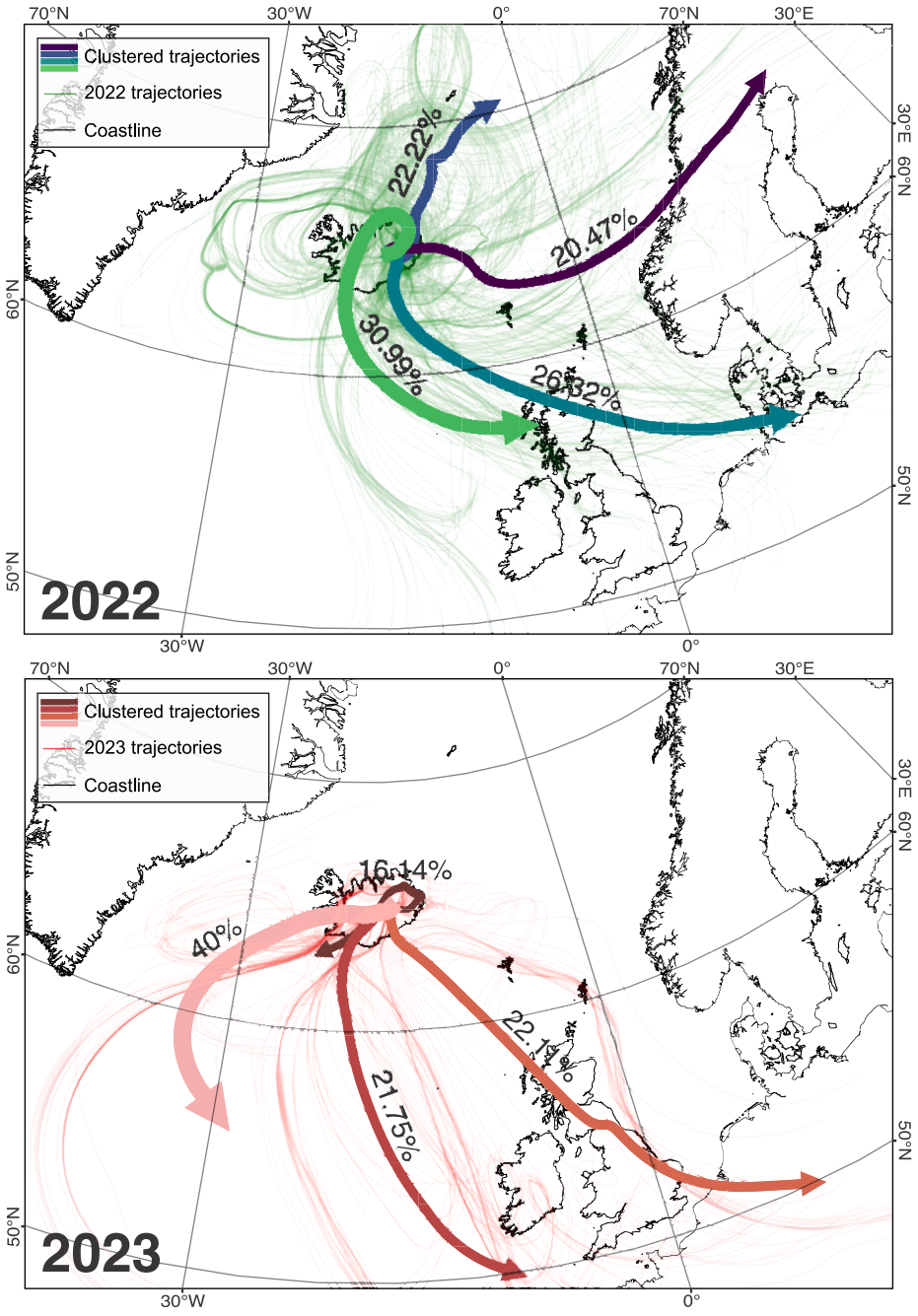

Fig. 7. Forward trajectory modelling using HYSPLIT. Modeled 5-day forward air parcel trajectories run hourly for the duration of the sampling periods in 2022 (top) and 2023 (bottom), starting at Dyngjusandur at 100 m altitude. Thin lines show individual trajectories (green: 2022, red: 2023), while thick colored arrows represent trajectory clusters with percentages indicating the proportion of total trajectories in each cluster.

The relationship between community structure and meteorological parameters provides evidence that airborne communities are shaped by deterministic processes. At Dyngjusandur, bioaerosol communities were consistently phylogenetically clustered according to NRI and NTI indices for both 16S and 18S datasets (Fig. 2), which typically is associated with strong environmental filtering (Stegen et al., 2012). NTI increased with maximum wind speed (Supplementary Material Table S2), suggesting more closely related taxa were released during storms, likely those associated with the sandsheet. Higher intensity storm conditions resulted in higher alpha diversity (Table 1) and increased beta diversity, with low-pressure samples being compositionally distinct from other bioaerosol samples (Fig. 5). These storm events likely facilitated the entrainment of a broader range of particle sizes (Fig. 4), thereby allowing a more diverse subset of the surface microbiome to enter the atmosphere. Similarly, in dusty environments elsewhere on Earth, certain taxa are strongly associated with dust storm events. For example, fungal abundances, particularly *Cladosporium*, increased during dust storm days in Taiwan (Ho et al., 2005). In contrast to these results, previous studies have demonstrated that in urban environments, pollutants affect the community structure and composition more than meteorological variables (Qi et al., 2020). While we did not measure atmospheric pollutants directly, our findings from Dyngjusandur suggest that, in the absence of substantial anthropogenic input, natural meteorological variability plays a key role in structuring atmospheric microbiomes. Therefore, proximity to anthropogenic activity is likely a primary control on the structure of atmospheric microbial communities

(Jiang et al., 2022).

Previous work has identified common sources of airborne bacteria, including soil, water bodies, vegetation, animal waste, and anthropogenic environments (Niu et al., 2023; Qi et al., 2020). Comparative analyses against the source environments at Dyngjusandur (sand, diurnal floodplains, and fluvial environments) revealed similar trends to these previous studies. For example, community dissimilarity between aerosol samples and local sources decreased during storm events, particularly with sand and, to a lesser extent, floodplain sources (Fig. 5; Table 2). The SourceTracker2 analysis corroborated this pattern. On days with strong gusts, aerosols were predominantly sourced from sand environments, with contributions from fluvial sources slightly increasing when wind speeds were lower (Fig. 3), presumably from bubble bursting (Michaud et al., 2018) or biofilm release (McDougald et al., 2012). Diurnal floodplain environments sourced a minor fraction of the microorganisms across all weather conditions (Fig. 3), consistent with the fewer cells observed on the lighter particles, presumably hyaloclastite loess (Fig. 6), which is expected to be at higher concentrations in the glacial outwash (Baratoux et al., 2011). Active dust emission was observed in the field from this region (Fig. 1c), where some samples contained a substantial fine particle fraction (<10 μm; Supplementary Fig. S4). It is also possible that free-floating cells (Hu et al., 2020) were emitted from the source environments independently of dust particles.

Despite contributions from local sources during storms, a substantial fraction of the atmospheric community could not be attributed to any sampled environment (Fig. 3), and statistical analysis of beta diversity demonstrated significant phylogenetic differentiation between airborne and surface communities (Supplementary Material Table S5). These findings confirm that bioaerosols maintain distinct community structures despite varying contributions from local sources, suggesting more complex origins and assembly processes. The substantial "unknown" fraction likely reflects the convergence of multiple atmospheric processes rather than methodological limitations. While insufficient sampling of source environments or sequencing artifacts and contaminant DNA could contribute to this pattern, our rigorous decontamination steps and the consistency of our findings with previous airborne studies in Iceland (Daussin et al., 2024, 2023) support the existence of a real, structured atmospheric community distinct from the surrounding sandsheet. Phylogenetic clustering analyses (Fig. 2) demonstrated that airborne communities are environmentally filtered rather than randomly sampled from the sources. Additional contributions likely came from gravitational settling from higher altitudes (Bryan et al., 2019), potentially explaining the unknown fraction on calmer days. Moreover, HYSPLIT backward trajectory analysis revealed that air parcels primarily came from the North Atlantic and eastern Greenland (Supplementary Material Fig. S11), suggesting that the distinct bioaerosol populations possibly originated from the ocean (e.g., from sea spray or bubble bursting; Michaud et al., 2018). The convergence of evidence from source tracking, beta diversity, and phylogenetic null modelling supports the interpretation that atmospheric communities at Dyngjusandur reflect a mixture of local surface emissions, background atmospheric populations from long-range transport, and unsampled local sources.

The major bacterial phyla identified in this work were similar to the taxa identified in several other air surveys of Iceland, such as Sphingomonadaceae, Micrococcaceae, and *Serratia* using both culturing and amplicon sequence approaches (Daussin et al., 2024, 2023). The eukaryotic composition showed the presence of fungi involved in biogeochemical processes, plant decomposition, and pathogenesis in plants and crops. However, the most abundant fungal populations observed here (e.g., Agaricales, *Amylocorticium*, and *Helotiales*) diverged from those detected in dust storms at low latitudes (Ho et al., 2005). The identification of Apicomplexa and other parasitic protists raises the possibility for long-range transport of pathogens via dust plumes originating from the sandsheet. Previous work has also identified spores of Apicomplexa in air samples in other deserts (Belilla et al., 2022). Additionally, the presence of these potentially pathogenic or agriculturally relevant taxa, including *Corynebacterium*, *Cladosporium*, and *Ascochyta*, underscores the need for further investigation into the public health and ecosystem impacts of dust-mediated microbial dispersal. This is especially pressing in the context of increasing dust emissions from Iceland due to glacial retreat (Bullard et al., 2016).

Samples analyzed for microscopy showed the presence of microorganisms and biofilm-like structures attached to these dust particles (Fig. 6). Moreover, cells were predominantly associated with darker toned, optically opaque particles (Fig. 6a–c), presumably basaltic sand. In contrast, fewer cells were associated with the lighter toned, transparent particles (Fig. 6d–f; Supplementary Material Fig. S7). This preferential association suggests that not all particles are equally effective as microbial carriers. The increased surface morphological complexity on the sand may offer more favorable sites for adhesion and protection from radiation and desiccating conditions in the atmosphere, consistent with previous work showing a higher number of cells on grains as opposed to free floating cells (Dong et al., 2022; Hu et al., 2020). These microscopy observations complement the phylogenetic clustering results (Fig. 2), since not all members of the surface community are equally likely to enter the atmosphere. Instead, community composition aloft may reflect both the physics of the entrainment of dust and the survival of microorganisms linked to certain types of particles.

Sediment transport modelling suggests that wind speeds during certain sampling periods were sufficient to loft both silt- and sand-sized particles, creating opportunities for microbes to hitchhike on mineral surfaces (Fig. 4). However, it is unclear whether the microorganisms survived beyond immediate emission. While we did not include direct measures of activity in this study, there has been progress in understanding whether the atmosphere exhibits the characteristics of a true ecosystem including metabolic activity, or if it simply is a passive dispersal medium (Lappan et al., 2024). Previous detections of adenosine triphosphate (ATP) in bioaerosols as well as bacteria possessing extreme environment tolerance confirmed that certain microorganisms have the capacity to persist up to the lower altitudes of the stratosphere (Bryan et al., 2019). Similarly, our drop plate culturing analysis confirmed that viable microorganisms can be recovered from airborne deposition and included taxa adapted to cold and oligotrophic environments (e.g., *Psychrobacter*, *Pseudomonas antarctica*), suggesting that some airborne microorganisms are physiologically equipped to endure harsh atmospheric conditions and possibly remain active (Supplementary Material Table S6).

The presence of viable, particle-associated microorganisms sourced from the sandsheet with potential ecological and public health implications raises questions about the geographic reach of these bioaerosol emissions. HYSPLIT forward trajectory models showed that air parcels originating from Dyngjusandur during the study period potentially arrived in major population centers in the United Kingdom, Continental Europe, Svalbard, and Greenland (Fig. 7). This suggests extensive potential for long-range atmospheric transport of microorganisms from this near-Arctic dust source. Future studies could integrate satellite-based dust observations to further validate modeled transport pathways and constrain emission timing. Additionally, standardized protocols for bioaerosol sampling in dust-emitting environments would further facilitate cross-study comparisons and support broader applications in dust monitoring. The presence of an atmospheric microbial population sourced from a variety of locations in the study area (Fig. 3) and the direct observation of microorganisms on particles (Fig. 6) indicates that dust, and therefore microbial populations can be emitted from the sandsheet, particularly on gusty days. These storm events likely act as a key coupling mechanism between surface microbial reservoirs and the atmosphere, enabling the episodic transport of microbial consortia, including potentially viable, pathogenic, and agriculturally relevant taxa, across Iceland and into downwind regions of Europe and the Arctic. This dispersal mechanism has important implications for regional biogeography, climate processes, and public health. As climate

shifts intensify extreme weather events and increase desertification, these findings support the emerging view of the atmosphere as both a conduit for microbial transport and an integral component of Earth's biosphere.

CRediT authorship contribution statement

Nathan Hadland: Writing – original draft, Visualization, Validation, Methodology, Investigation, Funding acquisition, Formal analysis, Conceptualization. **Christopher W. Hamilton:** Writing – review & editing, Supervision, Resources, Project administration, Investigation, Funding acquisition, Conceptualization. **Peter Schroedl:** Writing – review & editing, Methodology, Investigation, Funding acquisition. **Federica Calabrese:** Writing – review & editing, Methodology, Investigation. **Jeffery Marlow:** Writing – review & editing, Supervision, Resources. **Solange Duhamel:** Writing – review & editing, Supervision, Resources, Project administration, Methodology, Funding acquisition, Conceptualization.

Funding

Funding support was provided by the National Defense Science and Engineering Graduate (NDSEG) Fellowship Program to N.H., Lewis and Clark Fund for Exploration and Field Research in Astrobiology from the American Philosophical Society to N.H., The University of Arizona Graduate and Professional Student Council Travel Grant to N.H., Arizona Astrobiology Center Seed Grant to S.D. and N.H., Scialog (Heising–Simons Foundation) grant 2023–4652 to C.W.H., NASA grants 80NSSC23K0224 and 80NSSC25K7265 to J.M., and Fjällräven X Explorers Club Field Grant support to P.S.

Declaration of competing interest

The authors declare that they have no known competing financial interests or personal relationships that could have appeared to influence the work reported in this paper.

Acknowledgments

We thank Matthew Varnam, Joana Voigt, and Brett Carr for assistance in the field. We thank Snædís Björnsdóttir for logistical support and helpful conversations. Thank you to Vatnajökull National Park Service (Vatnajökulsþjóðgarður) for providing permission to work at Dyngjusandur.

Appendix A. Supplementary data

The supplementary material includes figures: (1) sequencing contaminants; (2) temporal variability of different weather parameters for the study period; (3) community composition at the phylum level for source environments; (4) particle sizes of sediment samples; (5) Venn diagram for overlapping ASVs between aerosols and source environments; (6) confocal microscopy images at different wavelengths to check for autofluorescence and chlorophyll; (7) box and whisker plot showing estimated cell counts for random fields of view of different particle types; (8) community composition at the phylum level for 16S and 18S datasets; (9) inferred metabolisms for the bioaerosols using FAPROTAX; (10) inferred pathways for the bioaerosols using PICRUSt2; (11) backwards trajectories from the HYSPLIT model; and (12) mantel correlogram for different environmental variables to support phylogenetic null modelling; The supplementary material also includes tables of: (1) sampling locations; (2) fixed effects models; (3) pairwise kruskal–wallis comparisons; (4) mantel correlations for beta diversity; (5) pairwise permanova comparisons; and (6) summary of cultures (PDF). Supplementary data to this article can be found online at https://doi.org/10.1016/j.scitotenv.2026.181659.

Data availability

Link to GenBank SRA was shared

Microbial Dispersal from a Hyperactive Sandsheet in the Icelandic Highlands (Original data) (NCBI GenBank)

References

Achterberg, E.P., Steigenberger, S., Marsay, C.M., LeMoigne, F.A.C., Painter, S.C., Baker, A.R., Connelly, D.P., Moore, C.M., Tagliabue, A., Tanhua, T., 2018. Iron biogeochemistry in the high latitude North Atlantic Ocean. Sci. Rep. 8, 1283. https://doi.org/10.1038/s41598-018-19472-1.

Arnalds, O., Dagsson-Waldhauserova, P., Olafsson, H., 2016. The Icelandic volcanic aeolian environment: processes and impacts — a review. Aeolian Res. 20, 176–195. https://doi.org/10.1016/j.aeolia.2016.01.004.

Azua-Bustos, A., González-Silva, C., Fernández-Martínez, M.Á., Arenas-Fajardo, C., Fonseca, R., Martín-Torres, F.J., Fernández-Sampedro, M., Fairén, A.G., Zorzano, M. P., 2019. Aeolian transport of viable microbial life across the Atacama Desert, Chile: implications for Mars. Sci. Rep. 9, 11024. https://doi.org/10.1038/s41598-019-47394-z.

Baddock, M.C., Mockford, T., Bullard, J.E., Thorsteinsson, T., 2017. Pathways of high-latitude dust in the North Atlantic. Earth Planet. Sci. Lett. 459, 170–182. https://doi.org/10.1016/j.epsl.2016.11.034.

Baratoux, D., Mangold, N., Arnalds, O., Bardintzeff, J.-M., Platevoët, B., Grégoire, M., Pinet, P., 2011. Volcanic sands of Iceland - diverse origins of aeolian sand deposits revealed at Dyngjusandur and Lambahraun. Earth Surf. Process. Landf. 36, 1789–1808. https://doi.org/10.1002/esp.2201.

Basapathi Raghavendra, J., Mathanlal, T., Zorzano, M.-P., Martin-Torres, J., 2023. An optimized active sampling procedure for aerobiological DNA studies. Sensors 23, 2836. https://doi.org/10.3390/s23052836.

Belilla, J., Iniesto, M., Moreira, D., Benzerara, K., Gérard, E., López-García, J.M., Kotopoulou, E., López-García, P., 2022. Active microbial airborne dispersal and biomorphs as confounding factors for life detection in the cell-degrading brines of the polyextreme Dallol geothermal field. mBio 13, e00307–e00322. https://doi.org/10.1128/mbio.00307-22.

Bolyen, E., Rideout, J.R., Dillon, M.R., Bokulich, N.A., Abnet, C.C., Al-Ghalith, G.A., Alexander, H., Alm, E.J., Arumugam, M., Asnicar, F., Bai, Y., Bisanz, J.E., Bittinger, K., Brejnrod, A., Brislawn, C.J., Brown, C.T., Callahan, B.J., Caraballo-Rodríguez, A.M., Chase, J., Cope, E.K., Da Silva, R., Diener, C., Dorrestein, P.C., Douglas, G.M., Durall, D.M., Duvallet, C., Edwardson, C.F., Ernst, M., Estaki, M., Fouquier, J., Gauglitz, J.M., Gibbons, S.M., Gibson, D.L., Gonzalez, A., Gorlick, K., Guo, J., Hillmann, B., Holmes, S., Holste, H., Huttenhower, C., Huttley, G.A., Janssen, S., Jarmusch, A.K., Jiang, L., Kaehler, B.D., Kang, K.B., Keefe, C.R., Keim, P., Kelley, S.T., Knights, D., Koester, I., Kosciolek, T., Kreps, J., Langille, M.G.I., Lee, J., Ley, R., Liu, Y.-X., Loftfield, E., Lozupone, C., Maher, M., Marotz, C., Martin, B.D., McDonald, D., McIver, L.J., Melnik, A.V., Metcalf, J.L., Morgan, S.C., Morton, J.T., Naimey, A.T., Navas-Molina, J.A., Nothias, L.F., Orchanian, S.B., Pearson, T., Peoples, S.L., Petras, D., Preuss, M.L., Pruesse, E., Rasmussen, L.B., Rivers, A., Robeson, M.S., Rosenthal, P., Segata, N., Shaffer, M., Shiffer, A., Sinha, R., Song, S.J., Spear, J.R., Swafford, A.D., Thompson, L.R., Torres, P.J., Trinh, P., Tripathi, A., Turnbaugh, P.J., Ul-Hasan, S., van der Hooft, J.J.J., Vargas, F., Vázquez-Baeza, Y., Vogtmann, E., von Hippel, M., Walters, W., Wan, Y., Wang, M., Warren, J., Weber, K. C., Williamson, C.H.D., Willis, A.D., Xu, Z.Z., Zaneveld, J.R., Zhang, Y., Zhu, Q., Knight, R., Caporaso, J.G., 2019. Reproducible, interactive, scalable and extensible microbiome data science using QIIME 2. Nat. Biotechnol. 37, 852–857. https://doi.org/10.1038/s41587-019-0209-9.

Bottos, E.M., Woo, A.C., Zawar-Reza, P., Pointing, S.B., Cary, S.C., 2014. Airborne bacterial populations above desert soils of the McMurdo dry valleys, Antarctica. Microb. Ecol. 67, 120–128. https://doi.org/10.1007/s00248-013-0296-y.

Bowers, R.M., McLetchie, S., Knight, R., Fierer, N., 2011. Spatial variability in airborne bacterial communities across land-use types and their relationship to the bacterial communities of potential source environments. ISME J. 5, 601–612. https://doi.org/10.1038/ismej.2010.167.

Bowers, R.M., Clements, N., Emerson, J.B., Wiedinmyer, C., Hannigan, M.P., Fierer, N., 2013. Seasonal variability in bacterial and fungal diversity of the near-surface atmosphere. Environ. Sci. Technol. 47, 12097–12106. https://doi.org/10.1021/es402970s.

Bryan, N.C., Christner, B.C., Guzik, T.G., Granger, D.J., Stewart, M.F., 2019. Abundance and survival of microbial aerosols in the troposphere and stratosphere. ISME J. 13, 2789–2799. https://doi.org/10.1038/s41396-019-0474-0.

Bullard, J.E., Baddock, M., Bradwell, T., Crusius, J., Darlington, E., Gaiero, D., Gassó, S., Gisladottir, G., Hodgkins, R., McCulloch, R., McKenna-Neuman, C., Mockford, T., Stewart, H., Thorsteinsson, T., 2016. High-latitude dust in the earth system. Rev. Geophys. 54, 447–485. https://doi.org/10.1002/2016RG000518.

Busse, H.-J., 2016. Review of the taxonomy of the genus *Arthrobacter*, emendation of the genus *Arthrobacter* sensu lato, proposal to reclassify selected species of the genus *Arthrobacter* in the novel genera *Glutamicibacter* gen. Nov., *Paeniglutamicibacter* gen. Nov., *Pseudoglutamicibacter* gen. Nov., *Paenarthrobacter* gen. Nov. and *Pseudarthrobacter* gen. Nov., and emended description of *Arthrobacter roseus*. Int. J. Syst. Evol. Microbiol. https://doi.org/10.1099/ijsem.0.000702.

Byloos, B., Maan, H., Van Houdt, R., Boon, N., Leys, N., 2018. The ability of basalt to leach nutrients and support growth of *Cupriavidus metallidurans* ch34 depends on

basalt composition and element release. Geomicrobiol J. 35, 438–446. https://doi.org/10.1080/01490451.2017.1392650.
Callahan, B.J., McMurdie, P.J., Rosen, M.J., Han, A.W., Johnson, A.J.A., Holmes, S.P., 2016. DADA2: high-resolution sample inference from Illumina amplicon data. Nat. Methods 13, 581–583. https://doi.org/10.1038/nmeth.3869.
Carotenuto, F., Georgiadis, T., Gioli, B., Leyronas, C., Morris, C.E., Nardino, M., Wohlfahrt, G., Miglietta, F., 2017. Measurements and modeling of surface–atmosphere exchange of microorganisms in Mediterranean grassland. Atmos. Chem. Phys. 17, 14919–14936. https://doi.org/10.5194/acp-17-14919-2017.
Dagsson-Waldhauserova, P., Arnalds, O., Olafsson, H., Hladil, J., Skala, R., Navratil, T., Chadimova, L., Meinander, O., 2015. Snow–dust storm: unique case study from Iceland, march 6–7, 2013. Aeolian Res. 16, 69–74. https://doi.org/10.1016/j.aeolia.2014.11.001.
Daussin, A., Vannier, P., Ménager, M., Daboussy, L., Šantl-Temkiv, T., Cockell, C., Marteinsson, V.Þ., 2023. Comparison of atmospheric and lithospheric culturable bacterial communities from two dissimilar active volcanic sites, Surtsey island and Fimmvörðuháls mountain in Iceland. Microorganisms 11, 665. https://doi.org/10.3390/microorganisms11030665.
Daussin, A., Vannier, P., Daboussy, L., Šantl-Temkiv, T., Cockell, C., Marteinsson, V.Þ., 2024. Atmospheric dispersal shapes rapid bacterial colonization of Icelandic lava rocks. FEMS Microbes 5, xtae016. https://doi.org/10.1093/femsmc/xtae016.
Davis, N.M., Proctor, D.M., Holmes, S.P., Relman, D.A., Callahan, B.J., 2018. Simple statistical identification and removal of contaminant sequences in marker-gene and metagenomics data. Microbiome 6, 226. https://doi.org/10.1186/s40168-018-0605-2.
de Araujo, G.G., Rodrigues, F., Gonçalves, F.L.T., Galante, D., 2019. Survival and ice nucleation activity of *pseudomonas syringae* strains exposed to simulated high-altitude atmospheric conditions. Sci. Rep. 9, 7768. https://doi.org/10.1038/s41598-019-44283-3.
De Frenne, P., Beugnon, R., Klinges, D., Lenoir, J., Niittynen, P., Pincebourde, S., Senior, R.A., Aalto, J., Chytrý, K., Gillingham, P.K., Greiser, C., Gril, E., Haesen, S., Kearney, M., Kopecký, M., le Roux, P.C., Luoto, M., Maclean, I., Man, M., Penczykowski, R., van den Brink, L., Van de Vondel, S., De Pauw, K., Lembrechts, J. J., Kemppinen, J., Van Meerbeek, K., 2025. Ten practical guidelines for microclimate research in terrestrial ecosystems. Methods Ecol. Evol. 16, 269–294. https://doi.org/10.1111/2041-210X.14476.
Dommergue, A., Amato, P., Tignat-Perrier, R., Magand, O., Thollot, A., Joly, M., Bouvier, L., Sellegri, K., Vogel, T., Sonke, J.E., Jaffrezo, J.L., Andrade, M., Moreno, I., Labuschagne, C., Martin, L., Zhang, Q., Larose, C., 2019. Methods to investigate the global atmospheric microbiome. Front. Microbiol. 10. https://doi.org/10.3389/fmicb.2019.00243.
Dong, X., Chen, B., Maki, T., Shi, G., Duan, M., Khalid, B., 2022. Characteristic changes of bioaerosols in Beijing and Tsogt-Ovoo during dust events. Front. Environ. Sci. 10, 795489. https://doi.org/10.3389/fenvs.2022.795489.
Douglas, G.M., Maffei, V.J., Zaneveld, J.R., Yurgel, S.N., Brown, J.R., Taylor, C.M., Huttenhower, C., Langille, M.G.I., 2020. PICRUSt2 for prediction of metagenome functions. Nat. Biotechnol. 38, 685–688. https://doi.org/10.1038/s41587-020-0548-6.
Duhamel, S., Jacquet, S., 2006. Flow cytometric analysis of bacteria- and virus-like particles in lake sediments. J. Microbiol. Methods 64, 316–332. https://doi.org/10.1016/j.mimet.2005.05.008.
Eisenhofer, R., Minich, J.J., Marotz, C., Cooper, A., Knight, R., Weyrich, L.S., 2019. Contamination in low microbial biomass microbiome studies: issues and recommendations. Trends Microbiol. 27, 105–117. https://doi.org/10.1016/j.tim.2018.11.003.
Elliott, T.L., Spalink, D., Larridon, I., Zuntini, A.R., Escudero, M., Hackel, J., Barrett, R.L., Martín-Bravo, S., Márquez-Corro, J.I., Granados Mendoza, C., Mashau, A.C., Romero-Soler, K.J., Zhigila, D.A., Gehrke, B., Andrino, C.O., Crayn, D.M., Vorontsova, M.S., Forest, F., Baker, W.J., Wilson, K.L., Simpson, D.A., Muasya, A.M., 2024. Global analysis of Poales diversification – parallel evolution in space and time into open and closed habitats. New Phytol. 242, 727–743. https://doi.org/10.1111/nph.19421.
Field, J.P., Pelletier, J.D., 2018. Controls on the aerodynamic roughness length and the grain-size dependence of aeolian sediment transport. Earth Surf. Process. Landf. 43, 2616–2626. https://doi.org/10.1002/esp.4420.
Fröhlich-Nowoisky, J., Kampf, C.J., Weber, B., Huffman, J.A., Pöhlker, C., Andreae, M. O., Lang-Yona, N., Burrows, S.M., Gunthe, S.S., Elbert, W., Su, H., Hoor, P., Thines, E., Hoffmann, T., Després, V.R., Pöschl, U., 2016. Bioaerosols in the earth system: climate, health, and ecosystem interactions. Atmos. Res. 182, 346–376. https://doi.org/10.1016/j.atmosres.2016.07.018.
Gulden, G., Hallgrimsson, H., 2000. The genera *Galerina* Earle and *Phaeogalera* Kiihner (Basidiomycetes, Agaricales) in Iceland. Acta Botanica Islandica 13, 3–54.
Gusareva, E.S., Acerbi, E., Lau, K.J.X., Luhung, I., Premkrishnan, B.N.V., Kolundžija, S., Purbojati, R.W., Wong, A., Houghton, J.N.I., Miller, D., Gaultier, N.E., Heinle, C.E., Clare, M.E., Vettath, V.K., Kee, C., Lim, S.B.Y., Chénard, C., Phung, W.J., Kushwaha, K.K., Nee, A.P., Putra, A., Panicker, D., Yanqing, K., Hwee, Y.Z., Lohar, S. R., Kuwata, M., Kim, H.L., Yang, L., Uchida, A., Drautz-Moses, D.I., Junqueira, A.C. M., Schuster, S.C., 2019. Microbial communities in the tropical air ecosystem follow a precise diel cycle. Proc. Natl. Acad. Sci. 116, 23299–23308. https://doi.org/10.1073/pnas.1908493116.
Hamza, Mbareche, Marc, Veillette, Bilodeau, Guillaume J., Caroline, Duchaine, 2018. Bioaerosol sampler choice should consider efficiency and ability of samplers to cover microbial diversity. Appl. Environ. Microbiol. 84. https://doi.org/10.1128/AEM.01589-18 e01589–18.
Hirano, S.S., Upper, C.D., 2000. Bacteria in the leaf ecosystem with emphasis on *pseudomonas syringae*—a pathogen, ice nucleus, and epiphyte. Microbiol. Mol. Biol. Rev. 64, 624–653. https://doi.org/10.1128/mmbr.64.3.624-653.2000.
Ho, H.-M., Rao, C.Y., Hsu, H.-H., Chiu, Y.-H., Liu, C.-M., Chao, H.J., 2005. Characteristics and determinants of ambient fungal spores in Hualien, Taiwan. Atmos. Environ. 39, 5839–5850. https://doi.org/10.1016/j.atmosenv.2005.06.034.
Hu, W., Murata, K., Fan, C., Huang, S., Matsusaki, H., Fu, P., Zhang, D., 2020. Abundance and viability of particle-attached and free-floating bacteria in dusty and nondusty air. Biogeosciences 17, 4477–4487. https://doi.org/10.5194/bg-17-4477-2020.
Hudziak, S.X., Ukstins, I., Peate, D., Whelley, P., Scheidt, S., Hamilton, C.W., 2025. Improving quantitative ventifact analysis for climate investigations using the Dyngjusandur sandsheet in Iceland as a planetary analogue. J. Geol. Soc. London 182, jgs2024-173. https://doi.org/10.1144/jgs2024-173.
Jiang, X., Wang, C., Guo, J., Hou, J., Guo, X., Zhang, H., Tan, J., Li, M., Li, X., Zhu, H., 2022. Global meta-analysis of airborne bacterial communities and associations with anthropogenic activities. Environ. Sci. Technol. 56, 9891–9902. https://doi.org/10.1021/acs.est.1c07923.
Jolly, E., 2018. Pymer4: connecting R and Python for linear mixed modeling. J. Open Source Software 3, 862.
Joung, Y.S., Ge, Z., Buie, C.R., 2017. Bioaerosol generation by raindrops on soil. Nat. Commun. 8, 14668. https://doi.org/10.1038/ncomms14668.
Karstens, L., Asquith, M., Davin, S., Fair, D., Gregory, W.T., Wolfe, A., Braun, J., McWeeney, S., 2019. Controlling for contaminants in low-biomass 16s rRNA gene sequencing experiments. mSystems 4, 10.1128/msystems.00290-19. https://doi.org/10.1128/msystems.00290-19.
Katoh, K., Misawa, K., Kuma, K., Miyata, T., 2002. MAFFT: a novel method for rapid multiple sequence alignment based on fast Fourier transform. Nucleic Acids Res. 30, 3059–3066. https://doi.org/10.1093/nar/gkf436.
Kellogg, C.A., Griffin, D.W., 2006. Aerobiology and the global transport of desert dust. Trends Ecol. Evol. 21, 638–644. https://doi.org/10.1016/j.tree.2006.07.004.
Kelly, L.C., Cockell, C.S., Thorsteinsson, T., Marteinsson, V., Stevenson, J., 2014. Pioneer microbial communities of the Fimmvörðuháls lava flow, Eyjafjallajökull, Iceland. Microb. Ecol. 68, 504–518. https://doi.org/10.1007/s00248-014-0432-3.
Kim, K.-H., Kabir, E., Jahan, S.A., 2018. Airborne bioaerosols and their impact on human health. J. Environ. Sci. 67, 23–35. https://doi.org/10.1016/j.jes.2017.08.027.
Knights, D., Kuczynski, J., Charlson, E.S., Zaneveld, J., Mozer, M.C., Collman, R.G., Bushman, F.D., Knight, R., Kelley, S.T., 2011. Bayesian community-wide culture-independent microbial source tracking. Nat. Methods 8, 761–765. https://doi.org/10.1038/nmeth.1650.
Lappan, R., Thakar, J., Molares Moncayo, L., Besser, A., Bradley, J.A., Goordial, J., Trembath-Reichert, E., Greening, C., 2024. The atmosphere: a transport medium or an active microbial ecosystem? ISME J. 18, wrae092. https://doi.org/10.1093/ismejo/wrae092.
Liu, C., Cui, Y., Li, X., Yao, M., 2021. Microeco: an R package for data mining in microbial community ecology. FEMS Microbiol. Ecol. 97, fiaa255. https://doi.org/10.1093/femsec/fiaa255.
Louca, S., Parfrey, L.W., Doebeli, M., 2016. Decoupling function and taxonomy in the global ocean microbiome. Science 353, 1272–1277. https://doi.org/10.1126/science.aaf4507.
Lozupone, C., Knight, R., 2005. Unifrac: a new phylogenetic method for comparing microbial communities. Appl. Environ. Microbiol. 71, 8228–8235. https://doi.org/10.1128/AEM.71.12.8228-8235.2005.
Martin, M., 2011. Cutadapt removes adapter sequences from high-throughput sequencing reads. EMBnet.journal 17, 10–12. https://doi.org/10.14806/ej.17.1.200.
Mayol, E., Arrieta, J.M., Jiménez, M.A., Martínez-Asensio, A., Garcias-Bonet, N., Dachs, J., González-Gaya, B., Royer, S.-J., Benítez-Barrios, V.M., Fraile-Nuez, E., Duarte, C.M., 2017. Long-range transport of airborne microbes over the global tropical and subtropical ocean. Nat. Commun. 8, 201. https://doi.org/10.1038/s41467-017-00110-9.
McDougald, D., Rice, S.A., Barraud, N., Steinberg, P.D., Kjelleberg, S., 2012. Should we stay or should we go: mechanisms and ecological consequences for biofilm dispersal. Nat. Rev. Microbiol. 10, 39–50. https://doi.org/10.1038/nrmicro2695.
Meinander, O., Kontu, A., Virkkula, A., Arola, A., Backman, L., Dagsson-Waldhauserová, P., Järvinen, O., Manninen, T., Svensson, J., de Leeuw, G., Leppäranta, M., 2014. Brief communication: light-absorbing impurities can reduce the density of melting snow. Cryosphere 8, 991–995. https://doi.org/10.5194/tc-8-991-2014.
Melosh, H.J., 2011. Wind. In: Planetary Surface Processes, Cambridge Planetary Science. Cambridge University Press, Cambridge, pp. 348–381. https://doi.org/10.1017/CBO9780511977848.010.
Michaud, J.M., Thompson, L.R., Kaul, D., Espinoza, J.L., Richter, R.A., Xu, Z.Z., Lee, C., Pham, K.M., Beall, C.M., Malfatti, F., Azam, F., Knight, R., Burkart, M.D., Dupont, C. L., Prather, K.A., 2018. Taxon-specific aerosolization of bacteria and viruses in an experimental ocean-atmosphere mesocosm. Nat. Commun. 9, 2017. https://doi.org/10.1038/s41467-018-04409-z.
Mountney, N.P., Russell, A.J., 2004. Sedimentology of cold-climate aeolian sandsheet deposits in the Askja region of Northeast Iceland. Sediment. Geol. 166, 223–244. https://doi.org/10.1016/j.sedgeo.2003.12.007.
Nakashima, M., Dagsson-Waldhauserová, P., 2019. A 60 year examination of dust day activity and its contributing factors from ten Icelandic weather stations from 1950 to 2009. Front. Earth Sci. 6, 245.
Neveu, M., Hays, L.E., Voytek, M.A., New, M.H., Schulte, M.D., 2018. The ladder of life detection. Astrobiology 18, 1375–1402. https://doi.org/10.1089/ast.2017.1773.
Niu, M., Huang, S., Hu, W., Wang, Y., Xu, W., Wei, W., Zhang, Q., Wang, Z., Zhang, D., Jin, R., Wu, L., Deng, J., Shen, F., Fu, P., 2023. Characteristics of bacterial and fungal communities and their associations with sugar compounds in atmospheric aerosols

at a rural site in northern China. Biogeosciences 20, 4915–4930. https://doi.org/10.5194/bg-20-4915-2023.
Pedersen, G.B.M., Höskuldsson, A., Dürig, T., Thordarson, T., Jónsdóttir, I., Riishuus, M. S., Óskarsson, B.V., Dumont, S., Magnusson, E., Gudmundsson, M.T., Sigmundsson, F., Drouin, V.J.P.B., Gallagher, C., Askew, R., Gudnason, J., Moreland, W.M., Nikkola, P., Reynolds, H.I., Schmith, J., 2017. Lava field evolution and emplacement dynamics of the 2014–2015 basaltic fissure eruption at Holuhraun, Iceland. J. Volcanol. Geotherm. Res. 340, 155–169. https://doi.org/10.1016/j.jvolgeores.2017.02.027.
Pointing, S.B., Belnap, J., 2012. Microbial colonization and controls in dryland systems. Nat. Rev. Microbiol. 10, 551–562. https://doi.org/10.1038/nrmicro2831.
Price, M.N., Dehal, P.S., Arkin, A.P., 2009. FastTree: computing large minimum evolution trees with profiles instead of a distance matrix. Mol. Biol. Evol. 26, 1641–1650. https://doi.org/10.1093/molbev/msp077.
Qi, Y., Li, Y., Xie, W., Lu, R., Mu, F., Bai, W., Du, S., 2020. Temporal-spatial variations of fungal composition in PM2.5 and source tracking of airborne fungi in mountainous and urban regions. Sci. Total Environ. 708, 135027. https://doi.org/10.1016/j.scitotenv.2019.135027.
Robeson II, M.S., O'Rourke, D.R., Kaehler, B.D., Ziemski, M., Dillon, M.R., Foster, J.T., Bokulich, N.A., 2021. RESCRIPt: Reproducible sequence taxonomy reference database management. PLoS Comput. Biol. 17, e1009581. https://doi.org/10.1371/journal.pcbi.1009581.
Ruiz-Gil, T., Acuña, J.J., Fujiyoshi, S., Tanaka, D., Noda, J., Maruyama, F., Jorquera, M. A., 2020. Airborne bacterial communities of outdoor environments and their associated influencing factors. Environ. Int. 145, 106156. https://doi.org/10.1016/j.envint.2020.106156.
Särkinen, T., Bohs, L., Olmstead, R.G., Knapp, S., 2013. A phylogenetic framework for evolutionary study of the nightshades (Solanaceae): a dated 1000-tip tree. BMC Evol. Biol. 13, 214. https://doi.org/10.1186/1471-2148-13-214.
Smith, D.J., Griffin, D.W., McPeters, R.D., Ward, P.D., Schuerger, A.C., 2011. Microbial survival in the stratosphere and implications for global dispersal. Aerobiologia 27, 319–332. https://doi.org/10.1007/s10453-011-9203-5.
Stegen, J.C., Lin, X., Konopka, A.E., Fredrickson, J.K., 2012. Stochastic and deterministic assembly processes in subsurface microbial communities. ISME J. 6, 1653–1664. https://doi.org/10.1038/ismej.2012.22.
Stein, A.F., Draxler, R.R., Rolph, G.D., Stunder, B.J.B., Cohen, M.D., Ngan, F., 2015. Noaa's HYSPLIT atmospheric transport and dispersion modeling system. Bull. Am. Meteorol. Soc. 96, 2059–2077. https://doi.org/10.1175/BAMS-D-14-00110.1.
Uetake, J., Tobo, Y., Uji, Y., Hill, T.C.J., DeMott, P.J., Kreidenweis, S.M., Misumi, R., 2019. Seasonal changes of airborne bacterial communities over Tokyo and influence of local meteorology. Front. Microbiol. 10, 1572. https://doi.org/10.3389/fmicb.2019.01572.
Warner, M.S.C., 2018. Introduction to PySPLIT: a Python toolkit for NOAA ARL'S HYSPLIT model. Comput. Sci. Eng. 20, 47–62. https://doi.org/10.1109/MCSE.2017.3301549.
Webb, C.O., Ackerly, D.D., McPeek, M.A., Donoghue, M.J., 2002. Phylogenies and community ecology. Annu. Rev. Ecol. Evol. Syst. 33, 475–505. https://doi.org/10.1146/annurev.ecolsys.33.010802.150448.
Weir-Brush, J.R., Garrison, V.H., Smith, G.W., Shinn, E.A., 2004. The relationship between gorgonian coral (Cnidaria: Gorgonacea) diseases and African dust storms. Aerobiologia 20, 119–126. https://doi.org/10.1023/B:AERO.0000032949.14023.3a.
Womack, A.M., Bohannan, B.J.M., Green, J.L., 2010. Biodiversity and biogeography of the atmosphere. Philos. Trans. R. Soc., B 365, 3645–3653. https://doi.org/10.1098/rstb.2010.0283.
Yarzábal, L.A., Salazar, L.M.B., Batista-García, R.A., 2021. Climate change, melting cryosphere and frozen pathogens: should we worry…? Environ. Sustain. 4, 489–501. https://doi.org/10.1007/s42398-021-00184-8.
Yilmaz, P., Parfrey, L.W., Yarza, P., Gerken, J., Pruesse, E., Quast, C., Schweer, T., Peplies, J., Ludwig, W., Glöckner, F.O., 2014. The SILVA and "all-species living tree project (LTP)" taxonomic frameworks. Nucleic Acids Res. 42, D643–D648. https://doi.org/10.1093/nar/gkt1209.
Zhang, B., Xu, Y., Yan, X., Pu, T., Wang, S., Yang, X., Yang, H., Zhang, G., Zhang, W., Chen, T., Liu, G., 2024. The diversity and risk of potential pathogenic bacteria on the surface of glaciers in the southeastern Tibetan plateau. Sci. Total Environ. 945, 173937. https://doi.org/10.1016/j.scitotenv.2024.173937.